EXAMINATION AND MATHEMATICAL MODELLING OF SHRINKAGE RATE OF UNIFORM DROPLETS IN A MICROFLUIDIC SYSTEM DESIGNED FOR BIOPRESERVATION

BİYOSAKLAMA AMACIYLA TASARLANAN MİKROAKIŞKAN DÜZENEKTE EŞBOYUTLU SULU DAMLACIKLARIN KÜÇÜLME HIZININ İNCELENMESİ VE MATEMATİKSEL MODELLENMESİ

UFUK OKUMUŞ

YRD. DOÇ. SELİS ÖNEL

Supervisor

Submitted to Institute of Sciences of Hacettepe University as a Partial Fulfillment to the Requirements for the Award of the Degree of Master of Science in Chemical Engineering

2015

To my dearest Sister, Pınar Okumuş

ETHICS

In this thesis study, prepared in accordance with the spelling rules of Institute of Graduate Studies in Science of Hacettepe University,

I declare that,

- all the information and documents have been obtained in the base of the academic rules
- all audio-visual and written information and results have been presented according to the rules of scientific ethics
- in case of using others Works, related studies have been cited in accordance with the scientific standards
- all cited studies have been fully referenced
- I did not do any distortion in the data set
- and any part of this thesis has not been presented as another thesis study at this or any other university.

12/06/2015

UFUK OKUMUŞ

ABSTRACT

EXAMINATION AND MATHEMATICAL MODELLING OF SHRINKAGE RATE OF UNIFORM DROPLETS IN A MICROFLUIDIC SYSTEM DESIGNED FOR BIOPRESERVATION

Ufuk OKUMUŞ

Master of Science, Department of Chemical Engineering

Supervisor: Asst. Prof. Selis ÖNEL

June 2015

Preserving biomaterials at low temperatures requires the use of carbohydrates as cryo-protective agents (CPAs) at high concentrations to increase the glass transition temperature, thus preventing the formation of extra- and intra-cellular ice formation at the cost of toxicity. In this thesis, we developed a mathematical model to investigate a microfluidic method proposed by Dr. Mehmet Toner for pre-concentration of cells with CPAs in continuous flow under fewer mechanical and osmotic stresses than traditional methods. New method is based on trapping cells into aqueous droplets and controlling the CPA concentration in the droplet by adjusting the temperature of the system. A water immiscible organic phase, which can solve small amounts of water, is utilized to remove water from the cell containing aqueous droplets. We solved the mathematical model based on two-phase flow and mass transfer through a moving boundary layer using Finite Element Analysis calculations on Comsol software together with external functions from MATLAB and Excel. The model showed that it is possible to pre-concentrate mammalian cells with CPAs to 10 times the initial concentration below 4 minutes via the BioMEMS based microfluidic method. We determined the critical droplet sizes for specific channel widths for optimum removal of water from the

aqueous droplets. Since membrane is the limiting media for diffusion, the CPA concentration should always be increased in a matched rate of diffusion through the cell membrane to avoid large concentration differences over the cell membrane. For a channel with a cross-section of 150 µm x 200 µm, the ideal initial aqueous droplet size to yield a maximum rate of increase in CPA concentration would be 90 microns. Finally, it is emphasized that, there is significant need for a mathematical model to include the volumetric response of the cell to concentration gradients ahead of the cell wall through an advanced model for diffusion through the cell membrane.

Keywords: Cryopreservation, BioMEMS, Cryo-Protective Agents, Transport Phenomena, Finite Element Analysis.

ÖZET

BİYOSAKLAMA AMACIYLA TASARLANAN MİKROAKIŞKAN DÜZENEKTE EŞBOYUTLU SULU DAMLACIKLARIN KÜÇÜLME HIZININ İNCELENMESİ VE MATEMATİKSEL MODELLENMESİ

Ufuk OKUMUŞ

**Yüksek Lisans, Kimya Mühendisliği Bölümü**

Tez Danışmanı: Yrd. Doç. Dr. Selis ÖNEL

Haziran 2015

Biyo-saklama günümüzde klinik tıp, doku mühendisliği, aşı, gıda, tarım ve kozmetik gibi alanlarda önemi giderek artan bir alandır. Biyo-saklama için çok çeşitli yöntemler uygulanmaktadır. Bunlar arasında canlı-dışı besi ortamında (in-vitro culture) saklama, düşük sıcaklıkta (hypothermic) saklama, dondurarak (cryopreservation) saklama ve kurutarak (dry-preservation) saklama sıralanabilir. Bu yöntemlerin kullanılmasındaki öncelikli amaç saklama öncesinde ve saklama süresince hücrede kalıcı bir hasar yaratmadan koruma sağlanmasıdır. Günümüzde dondurarak ve kurutarak saklama, özellikle hassas memeli hücrelerinin uzun süreli saklanması, üzerinde yoğunlukla çalışılması ve yeni yöntem ve teknolojiler geliştirilmesi gereken alanlardır. Bu yöntemler geliştirilirken örneklerin saklanması veya bir yerden bir yere taşınmasının da kolay ve düşük masraflı olması gözetilmek durumundadır. Dondurarak ve kurutarak saklama yöntemleri doğadaki örnekler izlenerek geliştirilmiştir. Bazı canlılar ortamdaki sıcaklık değişimleri veya donma/kuruma etkilerinin yarattığı gerilimlerin artmasıyla birlikte vücutlarında karbohidrat sentezler. Sentezlenen karbohidrat soğuk/kuraklık zamanında hücrenin zarar görmeden korunmasına olanak sağlar.

Memeli hücreleri evrimsel olarak kuru veya dondurarak saklamaya imkan verecek nitelikte gelişmemiştir. Bu koşulların yerine getirilmesi için koruyucu maddelerin dışarıdan eklenmesi gerekmektedir. Memeli hücreleriyle ilgili yapılan çalışmalar sonucu gliserol, trehaloz gibi karbohidratların düşük oranda kullanıldığı sürece uygun koruyucular olduğu tespit edilmiştir. Hücre içine giren karbohidratlar yüksek camsı geçiş sıcaklığına sahip olduğundan düşük sıcaklıklarda veya oda koşullarında vitrifiye ederek saklama imkanı sunmaktadır.

Hücrelerin vitrifiye edilmesinde en büyük engellerden biri donmaya karşı kullanılan ve camsı geçiş sıcaklığını yükseltmeye yarayan koruyucu kimyasallara yüksek derişimde ihtiyaç duyulmasıdır. Bu kimyasallara hücrenin uzun süre maruz kalması sonucu toksik etkilerinden dolayı hücreler zarar görmektedir. Dolayısı ile sistemin, camsılaşma öncesinde koruyucu madde etkilerine olabilecek en düşük sürede maruz kalması sağlanmalıdır. Bahsedilen etkiler koruyucu kimyasalların kontrollü biçimde hücreye verilmesiyle asgari boyutlara çekilebilir.
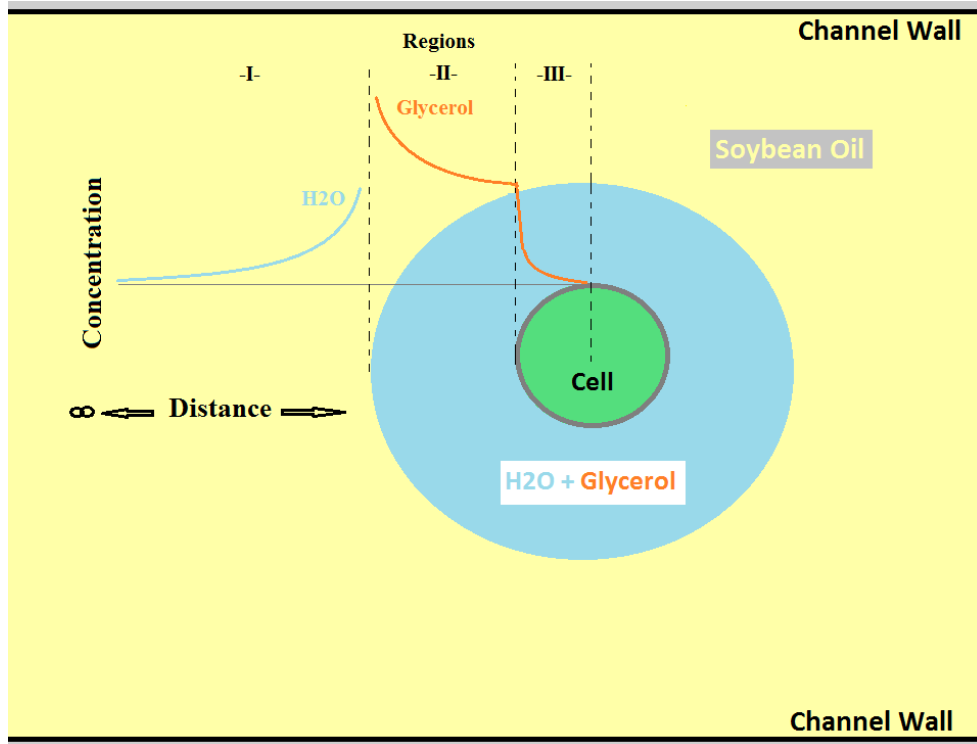
Şekil-1. Organik faz içerisinde sulu damlacığın ve hücrenin konumu ile beraber süreç içerisinde beklenen su ve koruyucu madde derişim eğrileri.

Çalışma kapsamında gliserol koruyucu madde olarak seçilmiştir. Ancak kurulan model hücre zarından geçebilen her madde için uygulanabilecek şekilde geliştirilmiştir. Çalışmada, sulu ortamda hücrelerin mikro-boyutlu küresel damlacıklar içinde hapsedilmesi sağlandıktan sonra sıcaklığa bağlı olarak organik fazın su çözünürlüğünün artması ile damlacıkların vitrifiye edilmesi için gerekli konsantrasyon değerine ulaşma koşulları incelenmiştir. **Şekil-1**'de kurulan sistemde tek bir damlacığın görünümü verilmiştir. Çalışmada suyun diğer faza yayınım hızı ve buna etki eden faktörler en önemli parametreler olarak öne çıkmaktadır.
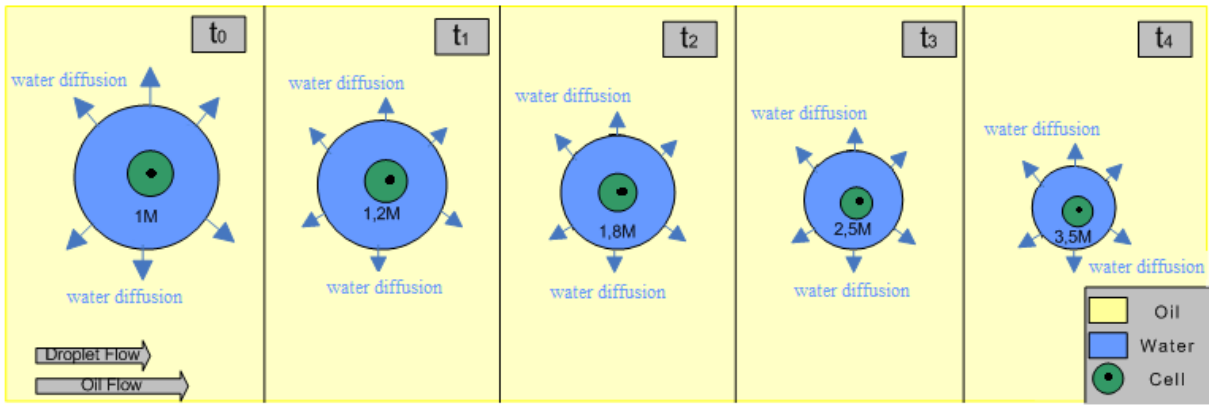
Şekil-2. Suyun organik faza salınımı sonucu tek bir damlacığın zaman içerisinde küçülüşü ve damlacık içerisindeki koruyucu madde derişiminin artışı.

Bu uygulamada diğer önemli husus genellikle yağlardan oluşan organik fazdır. Kütlece %0.3 miktarda suyu çözebilmesi, maliyeti düşük olması ve toksik etki yaratmaması soya yağını damlacık içindeki su miktarını sıcaklığa bağlı kontrol etmede ideal bir organik faz olarak öne çıkmaktadır.

Bu çalışmada bir mikro-akışkan sistemde oluşturulan eşboyutlu damlacıkların sıcaklığa ve dolayısı ile suyun organik faz icine yayınım hızına bağlı olarak küçülme hızı incelenirken, sulu damlacıkların içerdiği kimyasal derişiminin artışı incelenmek istenmektedir. Geleneksel dondurarak hücre saklama yöntemlerinde hücrelere koruyucu madde yükleme işi kademeli olarak yapılmaktadır. Kademeli olarak koruyucu madde yüklemek tek seferde koruyucu madde yüklemekten daha az zararlı olsa da, halen geliştirilmeye ihtiyacı vardır.

Çalışmada, Dr. Mehmet Toner'in araştırma grubu tarafından hücrelere CPA yüklenmesi amacı ile geliştirilen ve hücreleri düşük ozmotik basınca maruz bırakmayı amaçlayan bir mikro-akışkan düzenek incelenmiştir. İncelenen cihaz iki tane mikro kanalın birbiri ile dik olarak kesişmesinden oluşmaktadır. Akış sağlanırken aynı doğrultudaki iki kanaldan birbirine ters yönde yağ gönderilmektedir. Yağın gönderildiği kanallara dik olan üçüncü kanaldan ise daha düşük akış hızı ile su gönderilir. Su damlalar halinde doygun yağ fazına karışmadan geçer. Yağ akışının içinde oluşan su damlaları suyun akış yönünde itilerek dördüncü kanala doğru akar ve duzenli biçimde yağ içerisinde akan su damlaları elde edilir. Damlaların boyutu kanalların boyutlarına bağlı olarak değişirken, birim zamanda oluşan su damlacığı sayısı yağ ve suyun akış hızları ile bağlantılıdır. Düzeneğin yapımında özellikle yapışmayı önlemek amacı ile hidrofobik bir yüzey sağlayan poli-dimetil-siloksan (PDMS) tercih edilmiştir. PDMS'in bir başka özelliği olan şeffaflık ışık ve floresan mikroskopları ile analizlerinin yapılabilmesi açısından önem teşkil etmektedir.
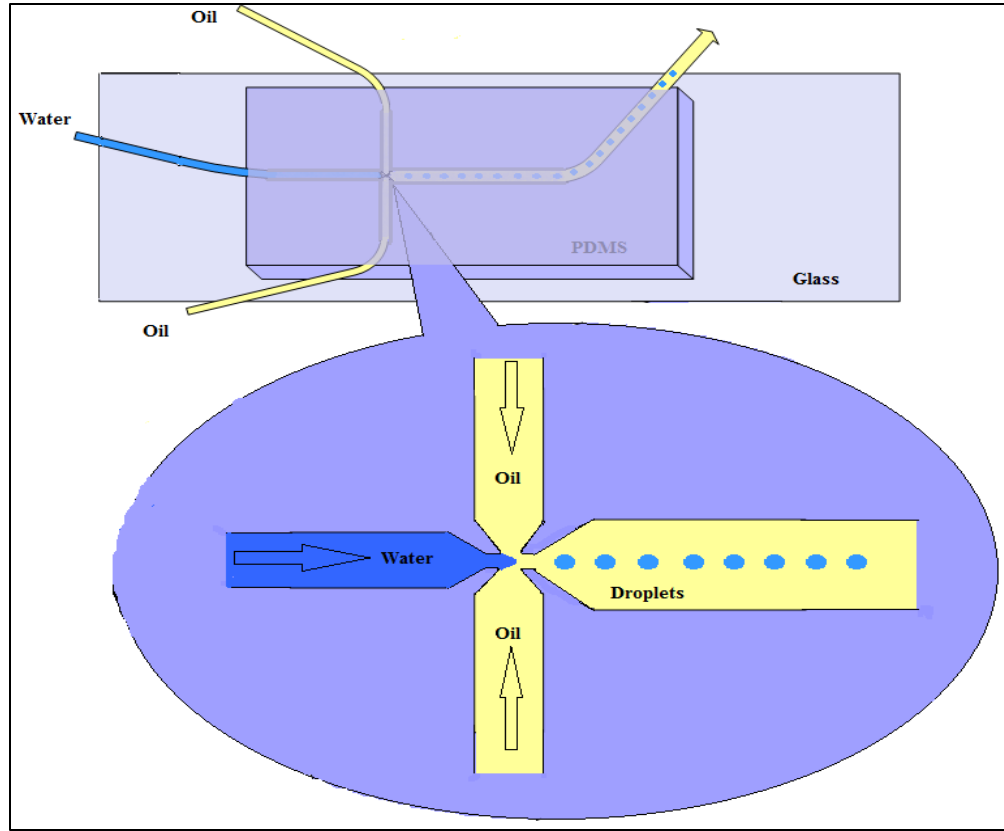
Şekil-3. Damlacıkların mikro-kanallarda oluşturulması ve PDMS'den yapılmış cihazın görüntüsü.

İncelenen sistem için matematiksel bir model geliştirilmiş damlacıkların küçülme hızı diğer parametrelere bağlı olarak gösterilmiştir. Çalışmada madde yayılımını matematiksel olarak tanımlamak için Fick madde dağınım yasası ve devamlılık denkleminden türetilmiş olan yığın taşınım ve difüzyon denkliği (convection-diffusion equation) kullanılmıştır. Akış dinamiklerini tanımlamak için Navier-Stokes denkliklerinin süreklilik versiyonlarından yararlanılmıştır. Akış profilini elde etmek için hareket denkleminden yararlanılmış, Reynold Sayısı 1'den küçük olduğu durumlarda geçerli olan laminar akış dinamikleri uygulanmıştır. Hücre zarından geçişin matematiksel açıklaması için bugün yaygın olarak kullanılan, ilk olarak 1932'de Jacobs M.H. tarafından ortaya atılan 2-parameter formalism (2 parametreli formalizm) modeli kullanılmıştır.

Bahsedilen matematiksel çözümlemeler Comsol Multiphysics yazılımı kullanılarak yapılmıştır. Buna ek olarak Comsol ile entegre veya uyumlu çalışabilmesinden dolayı MATLAB ve MS Excel yazılımları, basit kontrol hesapları ve değişkenlerin grafikler üzerinden ilişkilendirilmesi amacı ile kullanılmıştır. Matematiksel model **Şekil-6**'da verilen algoritma takip edilerek adım adım çözülmüştür.
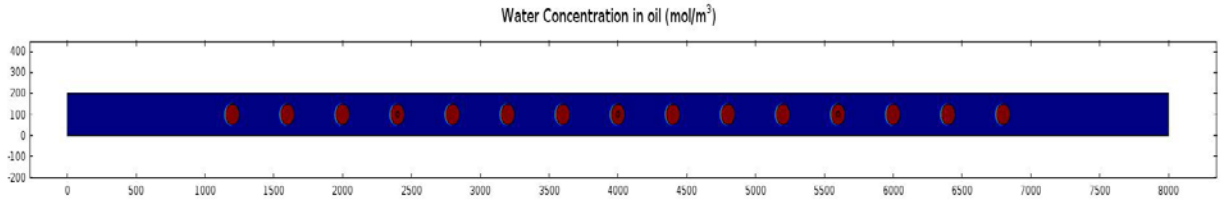
Şekil-4. Yağ içinde sulu faz akışının başlangıç koşullarında Comsol hesaplaması sonucu.
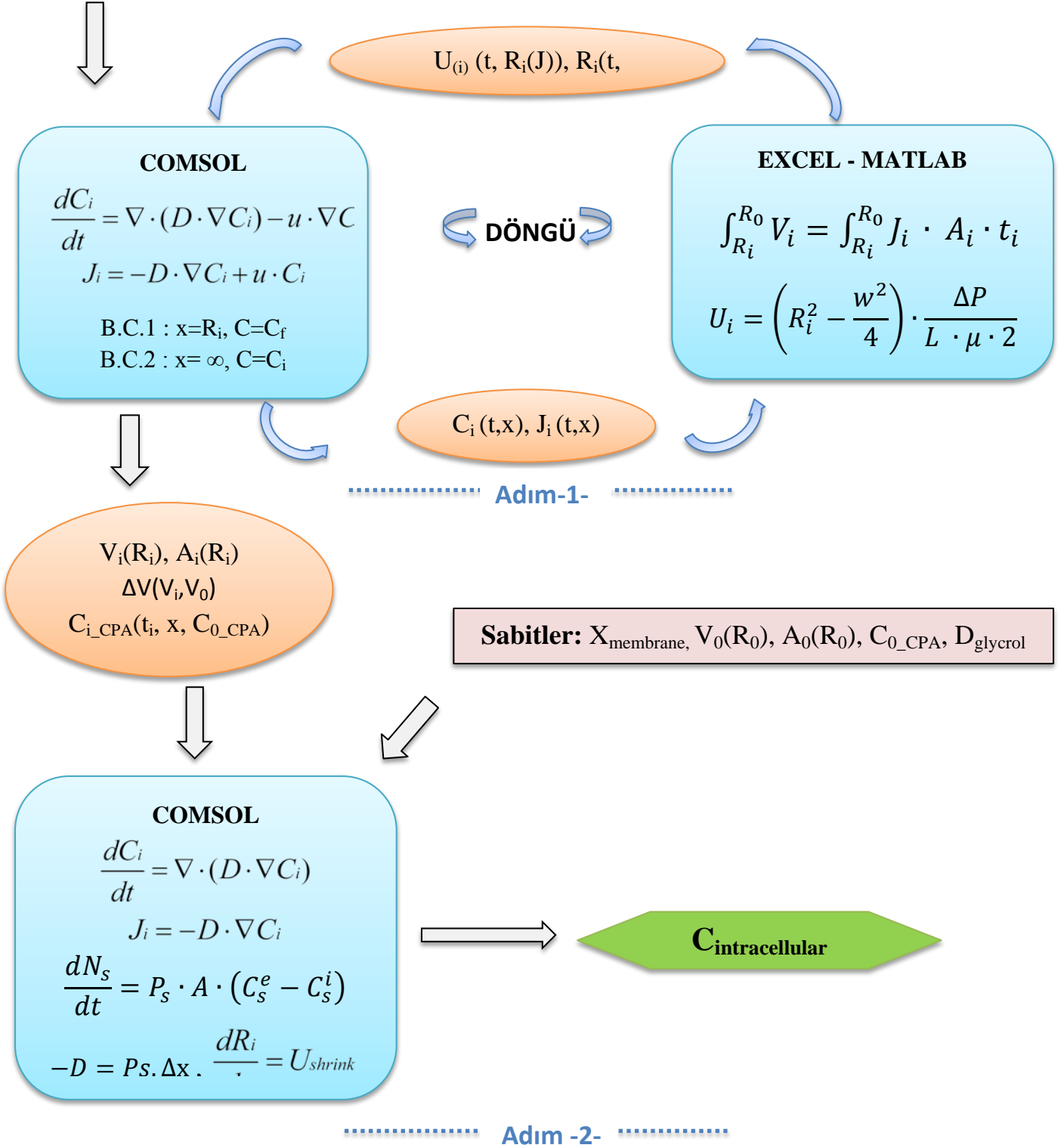
Kütle aktarımı Comsol Multiphysics yazılımı içerisinde bulunan Transport of Diluted Species modülü, akış dinamikleri Laminar Flow modülü, damlacıkların küçülmesi Moving Mesh modülü ile tanımlanmıştır. Ulaşılan akış ve derişim profilleri **Şekil-4** ve **Şekil-5**'de verilmiştir.
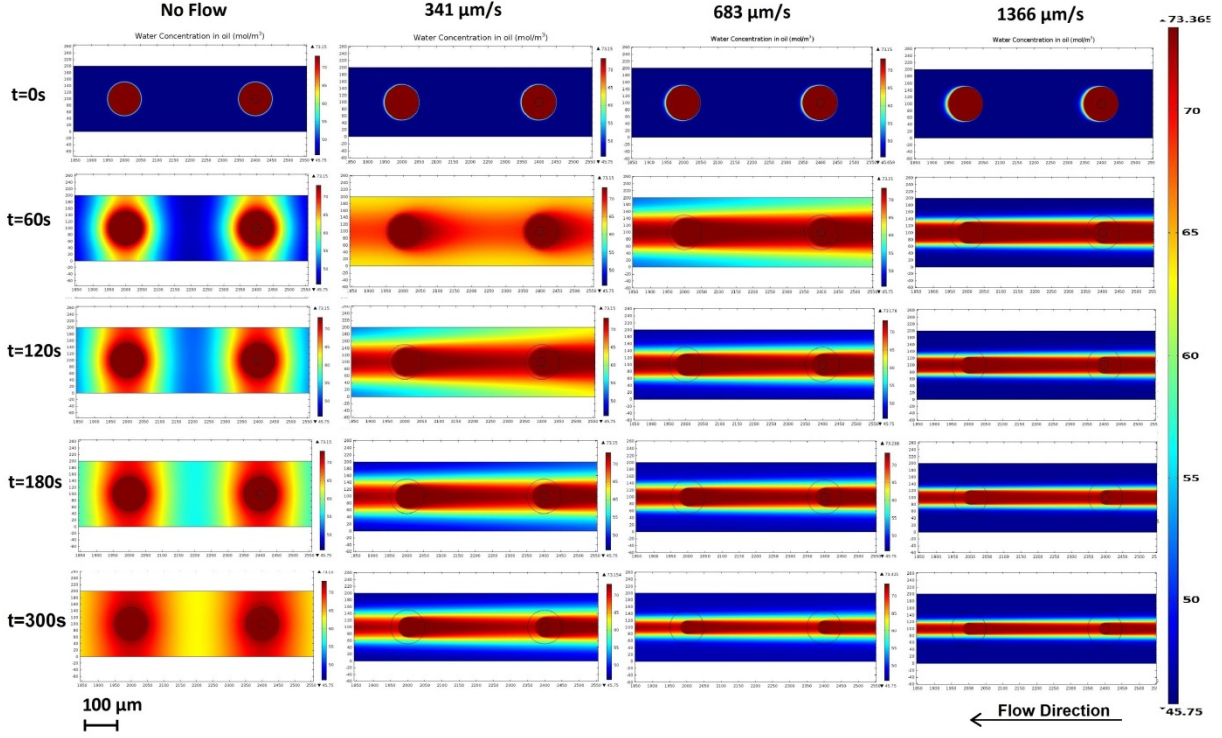
**Şekil-5**. Kurulan Comsol modelinin zaman içerisinde farklı akış hızlarında görüntüsü.

Sistemdeki değişkenlerden damlacık yarıçapı, damlacıklar ve organik fazın ortalama hızı arasındaki ilişkiyi anlatan bağıl hızı etkilemektedir. Bağıl hız, suyun organik faza geçiş akısını etkilemektedir. Akı ise, damlacık yarıçapın değişimini etkilemektedir. Bu döngüsel bağlantı ancak döngüsel bir hesaplama ile çözülebilmiştir. Buradan elde edilen sonuçlar damlacık içerisindeki derişimi bulmak için kullanılmış, daha sonra hücre zarından geçiş hesaplarıyla beraber hücre içi koruyucu madde derişimini veren $C_{intracellular}$ değişkeni bulunmuştur. Bu algoritma ve içerdiği denklikler **şekil-6**'da verilmiştir.

**Sabitler:** C_i, C_f, R_0, U_{avg}, ΔP, L, w, μ, D_{wtr}

$U_{(i)}(t, R_i(J))$, $R_i(t,$

COMSOL

$$\frac{dC_i}{dt} = \nabla \cdot (D \cdot \nabla C_i) - u \cdot \nabla C$$

$$J_i = -D \cdot \nabla C_i + u \cdot C_i$$

B.C.1 : $x = R_i$, $C = C_f$
B.C.2 : $x = \infty$, $C = C_i$

DÖNGÜ

EXCEL - MATLAB

$$\int_{R_i}^{R_0} V_i = \int_{R_i}^{R_0} J_i \cdot A_i \cdot t_i$$

$$U_i = \left(R_i^2 - \frac{w^2}{4} \right) \cdot \frac{\Delta P}{L \cdot \mu \cdot 2}$$

$C_i(t,x)$, $J_i(t,x)$

$\cdots$ **Adım-1-** $\cdots$

$V_i(R_i)$, $A_i(R_i)$
$\Delta V(V_i, V_0)$
$C_{i\_CPA}(t_i, x, C_{0\_CPA})$

Sabitler: $X_{membrane}$, $V_0(R_0)$, $A_0(R_0)$, C_{0_CPA}, $D_{glycrol}$

COMSOL

$$\frac{dC_i}{dt} = \nabla \cdot (D \cdot \nabla C_i)$$

$$J_i = -D \cdot \nabla C_i$$

$$\frac{dN_s}{dt} = P_s \cdot A \cdot \left(C_s^e - C_s^i \right)$$

$$-D = Ps.\Delta x \cdot \frac{dR_i}{\cdot} = U_{shrink}$$

$C_{intracellular}$

$\cdots$ **Adım -2-** $\cdots$

Şekil-6. Sistemin çözümünde izlenilen algoritma. Birinci adımda suyun organik faza geçişi ile ilgili değişkenler, ikinci adımda ise sulu damlacık içerisindeki derişim değişkenleri çözülmüştür.

Sonuç olarak, 150x200µm kesitli kanallar ile çalışılırken, 90 mikrondan küçük boyutlardaki sulu damlacıklar ile çalışılmasının en yüksek verimliliği sağlayacağı bulunmuştur. En iyi damlacık boyutu çalışma aralığı olarak 85 – 40 mikron aralığı bulunmuştur.
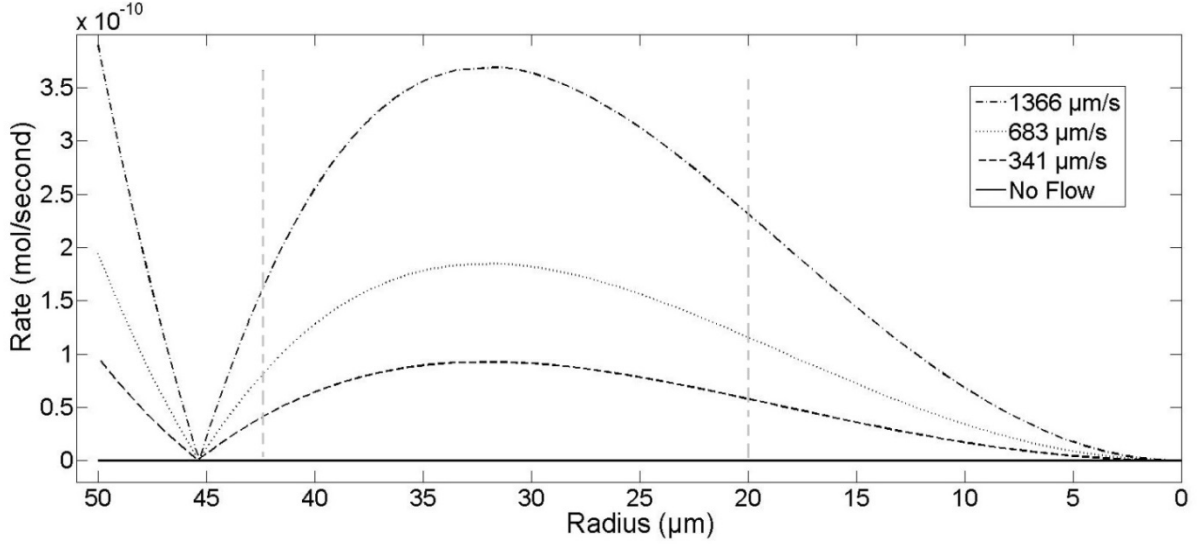
Şekil-7. Sulu damlacıktan organik faza madde aktarım hızı. Kesikli çizgiler en iyi aralığı göstermektedir.

85 mikron ile sürece başlandığında, teorik olarak, 300 saniyeden kısa sürede koruyucu madde başlangıç derişiminin 10 katına çıkarılabileceği görülmüştür. Akış hızının daha yüksek değerlere çekilmesinin kütle transfer hızını arttıracağı sonucuna varılmıştır. Ancak, bütün bu kütle transfer sisteminde sınırlayıcı yer hücre zarıdır. Damlacık içerisindeki derişim miktarı hızlı bir biçimde arttırılsa da, hücre zarından geçiş hızı derişimin artış hızını dengeleyecek biçimde artmayacaktır. Bu durum hücre zarının dışında madde birikimne yol açabilir ve hücrenin yüksek derişim farkına maruz kalması sonucu kullanılan cihazın amaçlarından biri olan hücreye düşük osmotik basınç uygulama söz konusu olmaktan çıkabilir. Sulu damlacık içerisindeki derişim artışı hücre zarından madde geçiş hızı ile uyumlu olacak seviyede tutulmalıdır. **Şekil-8** de incelenen sistemde derişimi arttırmak için teorik olarak geçmesi gereken süre verilmiştir.
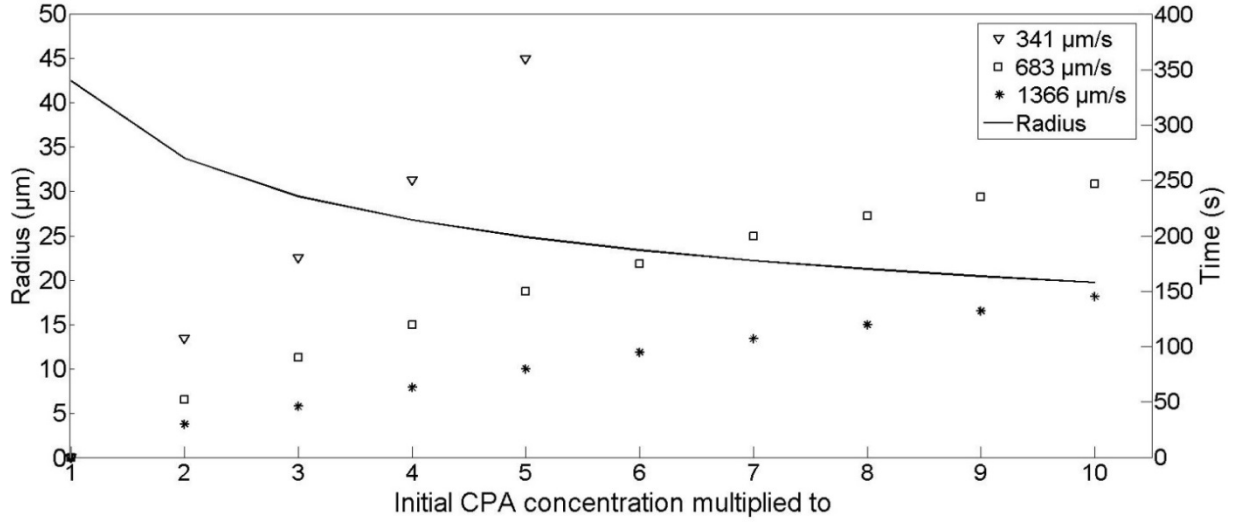
Şekil-8. 150 x 200μm kesitli kanalda, çeşitli hızlarda akan, 85 μm (42.5 μm yarıçap) boyutundaki damlacıklar için başlangıç derişiminin katlarına ulaşmak için gerekli süre.

Yazında hücre zarından madde geçişini tanımlayan teorik modeller bulunmaktadır. Çalışmamız sonucunda görülmüştür ki, hücrelerin ortamdaki derişim farklılıklarına vereceği tepkileri sürekli bir sistemde eksiksiz açıklayan bir model bulunmamaktadır. Yazındaki modeler ya hücre hacmini sabit kabul etmekte ya da değişen hücre hacminin hücre içi derişimi etkilemediğini kabul etmektedir. Deneysel verilerden bağımsız olarak hücrenin derişim farkına anlık olarak vereceği tepkiyi açıklayan bir modelin eksikliği farkedilmiş ve gelecekte araştırmaya değer bir konu olarak görülmüştür.

Anahtar Kelimeler: Biyosaklama, BioMEMS, Donmada Koruyucu Madde, Taşınım Olayları, Sonlu eleman analizi.

ACKNOWLEDGEMENTS

CONTENTS

LIST OF TABLES

LIST OF FIGURES

NOMENCLATURE

Latin

A	Area
B.C	Boundary Condition
C	Concentration
CPA	Cryoprotective Agent
D	Diffusion Coefficient
f	Body Forces
J	Flux
k	Convective Diffusion Coefficient
l	Characteristic length
L	Length
L_p	Hydraulic Conductivity
N_{RE}	Reynolds Number
N	Mass
N_s	Amount of Solute
N_{Sh}	Sherwood Number
P	Pressure
P_s	Solute Permeability
R_i	Radius (equal to y-coordinate on **eq.3**)
R	Universal Gas Constant
Rxn	Rate of reaction
T	Temperature
t	Time

u	Relative Velocity
Ui	Aqueous droplet velocity
v	linear velocity
V	Volume
V_w	Volume of Water
w	Width
x	Distance
Δx	Cell Membrane Thickness

Greek

μ	Viscosity
π	Osmolality
ρ	Density
σ	Reflection Coefficient

Subscripts

s	Permeating solute
n	Non-permeating solute
i	Time dependent (at any time)
0	Initial
f	Final

Superscripts

e	extracellular
i	intracellular

1. INTRODUCTION

Preservation and long term storage of cells is an essential need for many emerging cell based research, technologies and medical applications. There are different techniques to preserve a cell but they are referred to as 'biopreservation' for general speaking (Acker 2007). Biopreservation can be expressed as reversibly interrupting and suspending the vital activity of a living organism to hold stored in its non-native environment and vitalize it back later when organism is wanted to be biologically active again (M. Toner 2005). It is a naturally developed process by some microorganisms, however not naturally occurring in mammalian cells. Since mammalian cells are the most convenient tools to investigate mammalian organs and systems, they are in great importance for reparative medicine, cell biology of multicellular organisms and biochemistry related research. For instance, tissue engineering applications are mostly dependent on the cells and cell behaviors (Acker 2007). Without preserved and cultured mammalian cells, the only option is holding experiments on animals, which are expensive and very limited due to ethical reasons and cost of experiments. Hence, in vitro mammalian cell lines have served as widely used practical solution to this problem today.

There are several techniques to perform biopreservation. Some of them are hypothermic or cold preservation at relatively high (~4°C) temperatures, cryopreservation at very low (cryo) temperatures and desiccation (drying) at room temperature (Hammerstedt, Graham et al. 1990, Rubinsky 2003). All these techniques are focused on disabling chemical activity within the cell. The preferred preservation method is chosen by the criteria: How long the preservation will last, what kind of cell is going to be preserved or what the purpose of the preservation is. Cryopreservation comes to the forefront as the most reliable and favorable technique for biopreservation of mammalian cells.

A mammalian cell consists of organelles, a core with genetic material, cytoplasm and a membrane keeping everything inside. Cytoplasm content is ~50-70% water (Jerry W. King 1996, Illmer P 1999) allowing all the molecules within the cell to move freely for necessary chemical interactions to maintain vital activities. In a broad sense, 'water' or the 'cytoplasm' is the connection material between the organelles, core and outer environment of the cell.

From this point of view, if water is immobilized or completely removed from the cell, all the chemical activities, hence the vitality of the cell would be suspended. The immobilization process is possible only if certain conditions are provided (Michael J. Taylor 2004). One important condition is rapid cooling, which is based on removing heat so quick that molecules cannot move to form crystals. However, vitrification by rapid cooling is only possible if very high and costly rate of cooling (~10^6 $^\circ$C/s) is applied. Such cooling rates are currently not possible for biological materials. But, there is a way around this restriction by use of cryoprotectant agents (CPAs). CPAs are biocompatible substances, which penetrate between water molecules and limit the mobility of the water molecules. As a result, water can be immobilized at cooling rates lower than 10^6C/s. However, use CPAs cause lethal damages on the cell due to toxicity of CPAs at high concentrations. Conventional cryopreservation protocols utilize stepwise loading of CPAs into cells to expose cells to high concentrations as short time as possible. Yet, increasing concentration up to 6M, where slow cooling rates are practicable due to diffusion limitations, is resulting in low viability of cells due to toxicity.

A new method by which, the time scale of the process can be reduced and a continuous CPA loading process can be utilized to expose cells to lower osmotic stress by trapping cells into droplets was first developed at the BioMEMS Resource Center (Bajpayee, Edd et al. 2010). Involving microfluidic technology into this method to create a more stable and repeatable process as well as decreasing mechanical stress exerted on cells was the next step.

Bio Micro Electro Mechanical Systems (BioMEMS) technology is better than just an emerging technology now. It is being widely used in medicine, biotechnology, tissue engineering, electronics, qualitative analysis and many other researches related to health science or not (Ho, Lin et al. 2006, Chiu 2007, Jeffries, Kuo et al. 2007, Song, Moon et al. 2009, Sgro and Chiu 2010, Prot, Bunescu et al. 2012, Swain, Lai et al. 2013). Micro-channels and micro-wells in which reactions and physical changes take place are easy to monitor and control. They are continuous systems that allow for practical engineering solutions for production of chemicals, detection of trace amounts and examination of small droplets and reaction containers (Chiu 2007, Chiu, Lorenz et al. 2009).

Small micro-channels are capable of carrying cell containing aqueous droplets in an organic phase (He, Edgar et al. 2005, Chiu 2007, Chiu and Lorenz 2009, Sjostrom, Bai et al. 2014),

where, organic phase is a phase immiscible with water, yet has a capacity to solve water in small amounts. Changes in the temperature promote the solubility of water in organic phase, hence, allow us to control mass transfer of water between aqueous droplet and organic phase by controlling heat transfer (Bajpayee, Edd et al. 2010, Kuo and Chiu 2011). Here we make use of water loss of the aqueous droplets simply because decreasing water amount in a closed system increases the concentration of the remaining molecules. The important advantage of using continuous flow in a micro-device is that the increase in the concentration is a continuous and controlled change rather than a step change, and prevents the formation of harmful osmotic effects on mammalian cells (Song, Moon et al. 2009, Heo, Lee et al. 2011). This method is proposed to increase the viability of the cells after cryopreservation (Bajpayee, Edd et al. 2010, Heo, Lee et al. 2011).

Mathematical modeling and simulation of multi-physical systems allow for the testing of design and operational parameters of a system prior to manufacturing. Testing parameters during the design of the device provide the opportunity to prevent production of deficient designs, and to check experimental data with the mathematical calculations, creating more controlled and methodical work. In this thesis, we constructed a detailed multi-physics model of a microfluidic device originally created at the BioMEMS Resource Center for pre-concentration of cells. The device consists of two transparent rectangular micro-channels which are arranged to intersect and create a T-junction where the droplets are formed and directed into a wider channel as seen on **figure.3.2** and **figure 3.4**. We investigated the mass transfer in micro-droplets containing and not containing a cell and flowing in micro-channels, where convective and diffusive mass transfer mechanisms are taking place simultaneously between two phases. Also investigated outcomes of two phase fluid flow and mass transfer relation within the channel, where the aqueous droplets are flowing suspended within the organic phase. COMSOL Multiphysics software is used to create multi-physic models and MATLAB® and Excel functions are used to support and add extra mathematical expressions needed for the model. These software programs are processed simultaneously at certain stages of creating the eventual model. AutoCAD Engineering Design software is used to create the geometry of the system. We created an optimized model for understanding pre-concentration issues faced in cryopreservation of mammalian cells, in addition to creating a point of reference for future micro droplet applications made use in microfluidic devices.

2. THEORY

Microfluidics is a multidisciplinary research field including disciplines varying from fundamental physics to biology, electronics to chemistry. Design, shape and material of the microfluidic device may completely change depending on the purpose of use. In recent years, microfluidic devices are involved in many researches in wide variety of areas such as pharmaceutical industries or mammalian fertilization (Stone and Kim 2001, Swain, Lai et al. 2013). Here in this thesis BioMEMS and Bio-preservation oriented devices will be emphasized with an analyzed application of single cell droplet microfluidics.

2.1 Microfluidic Devices

Microfluidic devices were used to carry out molecular analysis methods; gas chromatography (GPC), high pressure liquid chromatography (HPLC) and capillary electrophoresis (CE). These micro-analytical methods have used microfluidic methods to make it possible to carry out high sensitivity analysis with very small amounts of samples. Capillary channels are utilized in these techniques. After achieving successful results researchers sought for improvements and various new applications (Whitesides 2006). One of these applications was developed in molecular biology. Sensitive microanalysis needed for genomics, DNA sequencing, has been partly maintained by microfluidic approaches (Whitesides 2006).

In 1990s, US Department of Defense has supported various researches on microfluidic devices to develop mobile detectors to protect their members in the field against chemical and biological threats. Co-operations with academy resulted in significant improvements in microfluidics technology (Whitesides 2006).

Another contribution came from silicon microelectronics. Some applications of photolithography and MEMS had been successful when applied to microfluidics in early periods (Czaplewski, Kameoka et al. 2003, Mijatovic, Eijkel et al. 2005). Later use of silicon in microfluidics was found inappropriate and mostly replaced with plastics like PDMS except for the use of silicon in rigid microfluidic device parts such as pumps or valves (Jessamine M. K. Ng 2002, Whitesides 2006).

In recent years, with the evolving technology automated systems with integrated electronic circuits have revolutionized our world from research labs to homes. As we get familiar with these systems a reasonable approach have been developed that if we can automate biological systems too? In fact, utilization of micro-channels is nothing new and microfluidic devices have been growing in importance as we identify more about micro-systems. Underlying physics in microfluidic systems are being widely studied to fulfill this purpose.

Today microfluidic devices are often referred to as micro electro mechanical systems (MEMS). After first use of micro-channels on chromatography devices, microfluidic devices have developed a lot and many other systems have integrated into micro devices. MEMS can be considered as very complicated devices with micro valves, electromagnetic micro tools and often with very complicated micro channel distributions and flow patterns. Of course all these tools have brought a new use for these systems (Weibel and Whitesides 2006, Whitesides 2006).

Development of microfluidic devices are in close relation with lithographical applications. Lithography is the main technique used to manufacture a micro device. Sensitivity level needed for production of micro-channels and micro-tools used within channels can only be achieved with a liable technique like lithography. During manufacture, patterns needed for micro-channels are maintained by use of surface lithography on a silicon wafer, and then molds for casting of structural polymer are produced with high sensitivity by using these patterns (Xia and Whitesides 1998). Casting is followed by a vacuum chamber and oxygen plasma on glass surface is used to fix the polymer on the glass slide. Usually several types of poly-dimethyl siloxane (PDMS) are used as polymer material for biological applications. Manufacturing of high pressure micro-devices also utilizes lithography but since more rigid materials are used in those devices, no molding is applied.

Micro channels naturally have very large surface area to fluid volume ratio compared to industrial macroscopic devices. This phenomenon gives microfluidic devices a characteristic flow pattern severely affected by surface tension. In a micro-channel flow is driven by only viscous forces and yielding flow regime is always perfectly laminar. This occasion causes mixing issues to become a whole new topic to be focused on while bringing a lot of new use

for these systems (Stroock, Dertinger et al. 2002). Further information on flow characteristics is given in section **2.4** fluid dynamics in micro-channels.

Microfluidic devices are being used for very high velocity applications using silicon and glass as the structural material. High pressure and velocity can be achieved in these systems. Hence, applications towards micro-reactors are often utilized in such systems when pressure increases the selectivity of the yielding reaction product (Elvira, Casadevall i Solvas et al. 2013).

MEMS that are developed for biological applications, referred to as BioMEMS, have been used in fields ranging from cryopreservation to fertilization, proteins to genetic researches (Squires and Quake 2005, Dittrich and Manz 2006, Chiu and Lorenz 2009, Song, Moon et al. 2009). Droplets generated in micro-channels are used as single reaction containers and many other applications sensitive to concentration including protein nucleation, crystallization and macromolecular crowding are under-research or on post-research phase for micro droplets flowing in micro-channels (Beebe, Mensing et al. 2002, He, Sun et al. 2004, Chiu 2007, Jeffries, Kuo et al. 2007, Chiu, Lorenz et al. 2009, Bajpayee, Edd et al. 2010, Lagus and Edd 2013).

Mainly, the greatest advantage brought by microfluidic devices is the existence of flow. Biological applications are often conducted on petri dishes where no regular predictable flow can be used. In micro-channels, biological organisms of couple of microns wide can be monitored as accurate as they were in petri dishes with the addition of flow when needed. Occurrence of flow can promote mass transfer greatly, separation can be done with the aid of flow, and a closed environment can be maintained whenever necessary. Two phase flow can be utilized to create precipitations or needed confined areas to perform detailed analysis (Kenis 1999, He, Sun et al. 2004). The only disadvantage of microfluidic devices is their cost as they usually must be specific to application with a unique pattern for each device.

Silicon and glass have been used in microfluidic devices in the early periods of development as acts of the influences came from the microelectronics technology applications. Later, polydimethylsiloxane (PDMS) and similar plastics have replaced the use of silicon in microfluidics. Silicon parts are still in use for valves and pumps and other rigid components of the microfluidic system but main structure consists of plastics and polymers today (Jessamine

M. K. Ng 2002). Silicon is more expensive and not transparent to ultra-violet or visible light. This downside of silicon prevents use of optical methods of detection over microfluidic devices (Whitesides 2006).

2.2 Cryopreservation

Cryopreservation, as the most successful preservation method to date, has been used widely as part of cancer and root cell research to protect and store mammalian cells despite complications. The cell cytoplasm that surrounds the organelles is mostly composed of water causing undesired results during freezing, such as expansion, extracellular ice formation, crystallization, and local increase in solute concentration due to crystallization (Toner, Cravalho et al. 1990). Crystallization and other solute effects can be prevented by vitrification of cell cytoplasm. Vitrification process depends on the molecular mobility, defined as the temperature and concentration dependent behavior of the water molecules and other ions in the cytoplasm. When cooling is under progress, if the mass transfer rate of water within the cell is high, then the cell will most likely suffer dehydration. If mass transfer rate of water is low enough, which is possible with ultra-fast cooling (10^6-10^7 C/s), then the cell cytoplasm can undergo vitrification suspending the mobility of any intracellular molecule (A. Aksan and M. Toner (M. Toner 2005)). During vitrification, the rate of heat transfer must be high enough to prevent any mass transfer that would form harmful crystals. With such high cooling rates water can be vitrified at -135 C. Unfortunately, ultrafast cooling is currently not possible for biological materials. Even so, reduction of rate of mass transfer within the cell cytoplasm is possible. Aforementioned damage to the cell can be eliminated by increasing glass transition temperature via introduction of cryo-protectant agent (CPA) carbohydrates such as glycerol into the cell (Meryman 1971, Eroglu, Russo et al. 2000). With the aid of CPAs, ratio of heat transfer rate to mass transfer rate can be held at reasonable levels (M. Toner 2005). This mechanism is naturally being used by some multicellular organisms. 'Tardigrade', an organism that can stand almost any condition, can replace its intracellular water with sugar trehalose and survive freezing by preventing crystallization (Crowe and Crowe 2000). However, mammalian cells do not possess such ability. Exposure to high concentrations of CPAs induces toxic effects and causes damage to the cell due to osmotic stresses and

shrinkage. To employ cryopreservation, special process must be implemented (Youm, Lee et al. 2014).

Currently, cryopreservation protocols include exposing of cells to relatively sudden changes of CPA concentrations to render them take CPA into cells (Youm, Lee et al. 2014). Cells respond to these changes in a way they would damage their organelles causing lethal damage to the whole cell in the end. To prevent lethal conditions, CPA concentration in cells is increased step by step. For instance; in the first step, cells are immersed in a 0.5 M CPA solution and kept there for couple of minutes and then taken into 1M CPA solution and kept there for a while and this process goes on until desired CPA concentration is reached within the cell. In addition to osmotic stress, all these steps put cells under a lot of mechanical stress with use of volume pipettes. Although yet, mammalian cells can stand all these processes, considering additional damage by the toxicity when cells are exposed to CPAs for too long, viability of cells are reduced in considerable amounts during all the rush of the pre-concentration process. A method that puts cells under less osmotic and mechanical stress in optimized time scales would fairly increase viability of cells.
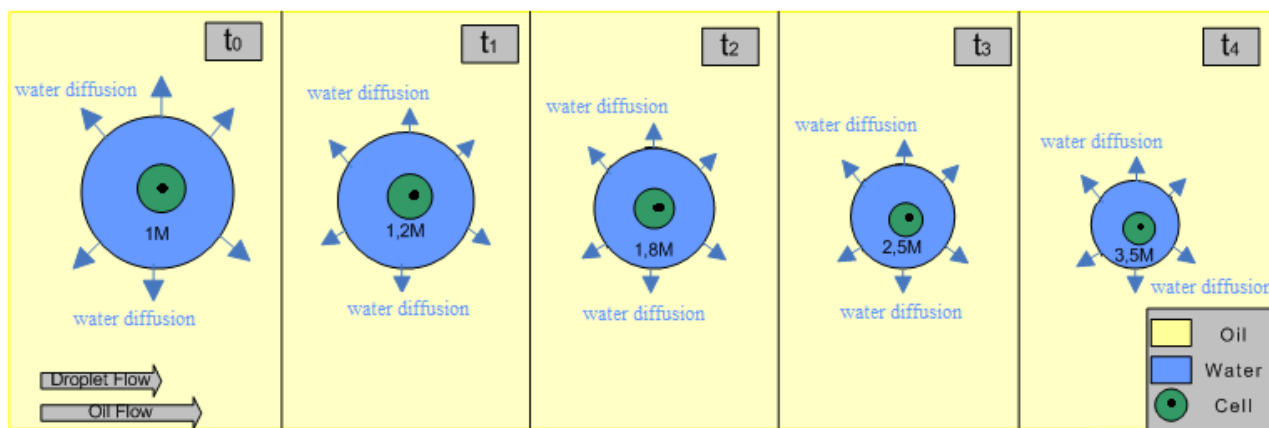
Figure 2.1 - Schematic representation of droplet shrinkage in microfluidic channel and water diffusion into organic phase yielding gradual increase in CPA concentration.

The rate and amount of CPA loading to the cell can be adjusted by controlling the CPA concentration through adjusting the amount of water around the cell. In this research, a CPA loading protocol proposed by Dr. Mehmet Toner is mathematically modeled for a thermal

micro-channel fluidic system, where controlled continuous increase in CPA concentration profile is enforced. **Figure.2.1** is a schematic representation of proposed method for pre-concentration of cells. The new system allows for encapsulation of cells in an aqueous droplet at low CPA concentration and gradual increase of CPA concentration by removal of water from the aqueous droplet into a continuously flowing immiscible organic phase. Soybean oil is employed as the organic phase due to limited solubility of water (~0.3 % by volume (He, Sun et al. 2004)) that is sufficient to achieve the desired aqueous droplet volume by diffusion of water into the thermally controlled oil.

A comparison can be seen on **figure.2.2** which summarizes application of traditional pre-concentration method (stepwise) and proposed methods (progressive). A smooth transition of CPA concentration will create less potential for damaging cells due to osmotic effects. The distinction of work on figure.2.3A and figure.2.3B is the utilization of droplets to create surrounding (buffer) environment for cells. This occasion decreases the potential of osmotic damages on sensitive cells by starting with a low increase ratio of CPA concentration and increase gradually with time.
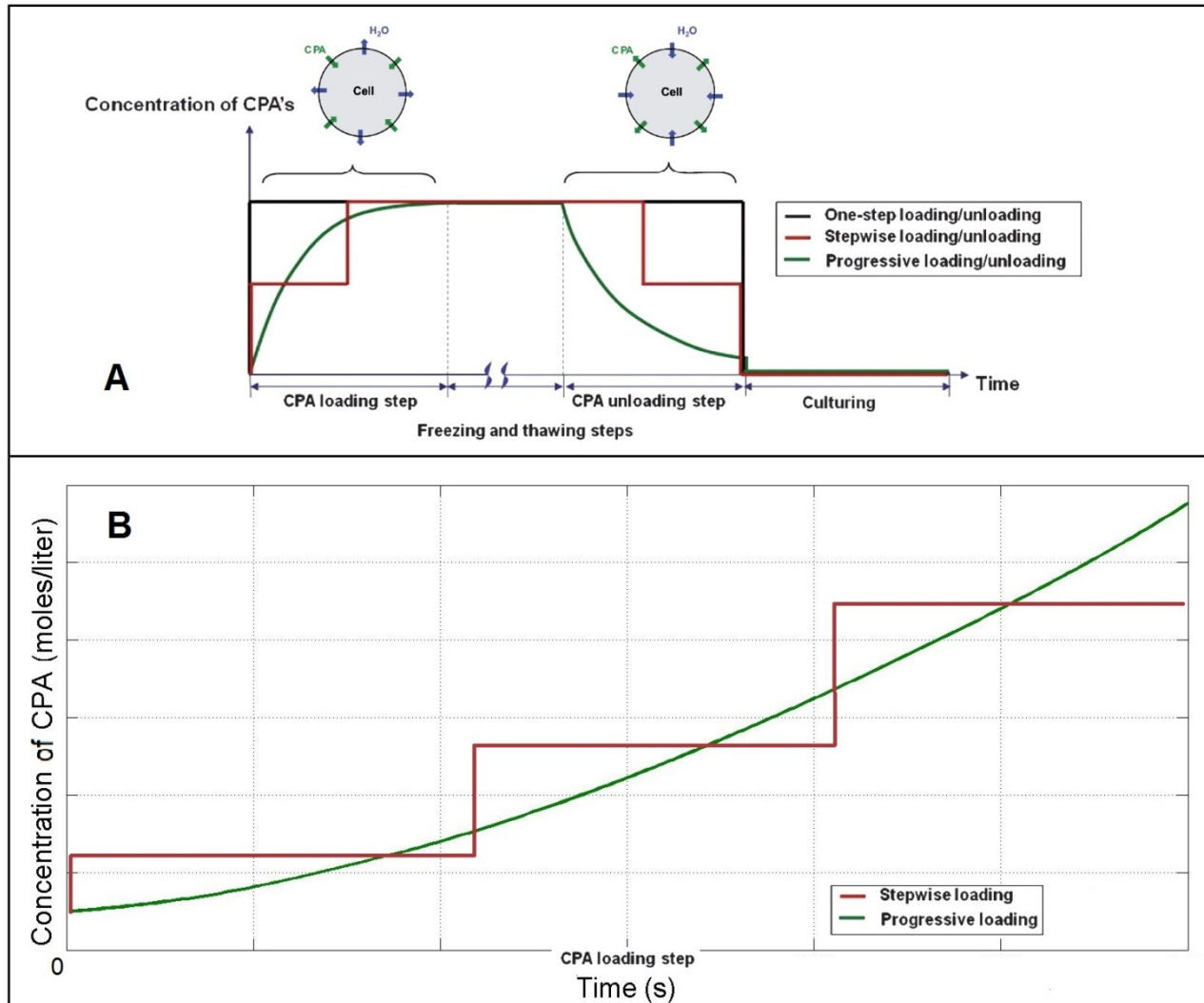
Figure.2.2 – (A) Distinction between stepwise loading/unloading and gradual (progressive) loading/unloading of CPA into cell (Song, Moon et al. 2009). **(B)** Distinction between stepwise loading and progressive loading in continuous flow of aqueous droplets.

2.3 Modeling and Simulation

The numerical solution of the mathematical model developed in this study is conducted by finite element analysis (FEA) method. FEA is used for solving differential equations in limited partitions with respect to given boundary conditions. In this method, a continuous physical problem is divided into very small nodal discontinuous physical partitions (see **figure.2.3**). Each partition is solved with respect to given boundary conditions and found

results are chosen as new boundary condition for the neighboring partitions until all system is solved. Step by step, each small sub system is solved by simple convergence functions (Hou and Efendiev 2009). Size of the partitions, so called finite elements, determines the sensitivity of the solution. Element size is distributed with respect to needed sensitivity within the physical system. Higher number of element yields more accurate results while it creates a larger work load on processors and takes longer time to work out. Hence, element size and accuracy must be handled well to avoid bad results or long time analysis course up to several days. In our study, finite element analysis calculations are carried on Comsol Multiphysics software. Other calculations of intermediate parameters and curve fits are conducted on MATLAB and MS Excel.
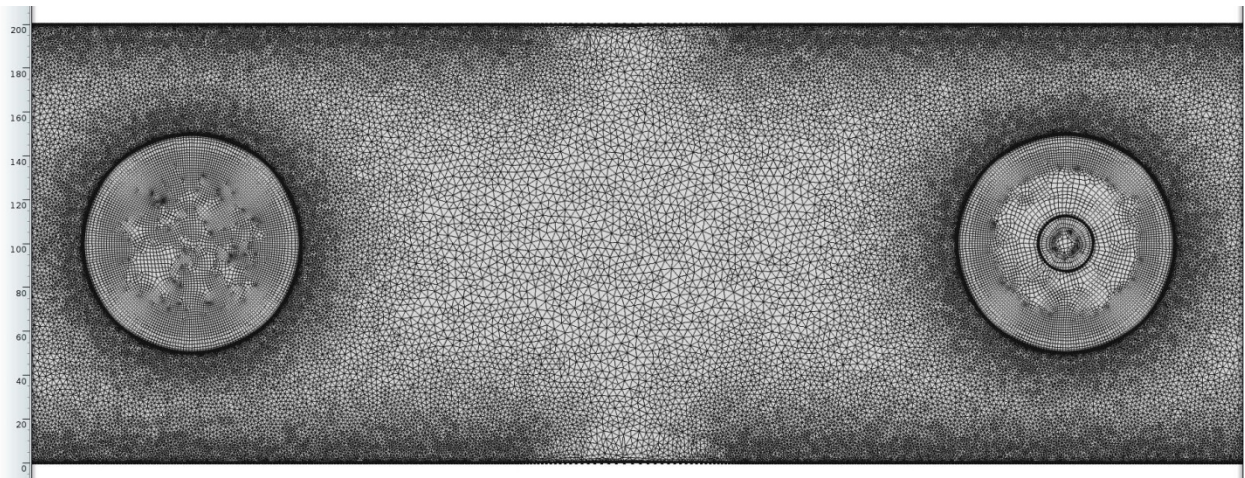
Figure.2.3- A part of the system showing finite elements generated on Comsol Multiphysics software.

Another important factor is the element size quality, also referred to as the mesh quality. It is a geometrical measure to define the capability of an element to perform desired calculations (Pryor 2011). It is scaled between 0 and 1, from bad to good, respectively. Element quality can be considered as a measure of how good an element fits into a circle. An element with high quality would fill larger portion of the circle than a lower quality element (Pryor 2011). This explains the element quality histograms shown on **figure.2.4**. The microfluidic system we modeled has triangular or quadrilateral elements with quality close to 1. Near the boundaries one must use thin quadrilateral elements, which characteristically have low element quality. This is the reason why there are low quality elements on the element quality

11

histogram on the left side of **figure.2.4**. Use of thin boundary layers was a necessity in this study to obtain a robust stretching element for the moving boundary on droplet walls.

Statistics	Statistics
Complete mesh	**Complete mesh**
Element type: All elements	Element type: Triangular elements
Triangular elements: 752890	Triangular elements: 752890
Quadrilateral elements: 189801	
Edge elements: 12718	Element statistics
Vertex elements: 76	Minimum element quality: 0.009904
Domain element statistics	Average element quality: 0.8881
	Element area ratio: 0.002271
Number of elements: 942691	Mesh area: 1467000.0 μm^2
Minimum element quality: 0.006569	
Average element quality: 0.805	
Element area ratio: 3.325E-4	
Mesh area: 1600000.0 μm^2	
Maximum growth rate: 12.63	
Average growth rate: 1.397	

Element Quality Histogram | **Element Quality Histogram**

Figure.2.4 - Mesh statistics for the calculations.

2.4 Transport Phenomena in Microfluidic Systems with Two Phase Flow

Flow characteristics of fluids running through a rectangular channel may vary depending on the dimensions of the channel. Fundamentals of fluid dynamics in large channels are pretty much realized now. In micro scale, fundamental physics may act different than that in large scale observations (Squires and Quake 2005, Janasek, Franzke et al. 2006). The effect, thus, the importance of inertial forces is much higher than viscous forces in large scale systems. This phenomenon allows fluid to mix easily with eddies and turbulence. In microsystems,

fluids do not mix convectively. Viscous forces override in significance. Chaotic mixing within the fluid flow is not at stake. For such liquids like water, laminar flow forms and maintains itself within the micro-channel. Occurrence of continuous laminar flow requires specific equipment to perform mixing within the micro-channel. Nevertheless, laminar flow has many advantages in various applications of microfluidic systems (Santiago 2001, Whitesides 2006).

Flow characteristics of a Newtonian fluid can be described by the Navier-Stokes equation given by:

$$\rho \left(\frac{\partial u}{\partial t} + u \cdot \nabla u \right) = -\nabla p + \mu \nabla^2 u + f \qquad \textbf{(eq.1)}$$

which is basically the continuum version of Newton's law of motion, F = m.a, on a per unit volume basis. In **eq.1**, u represents the velocity field, t time, σ fluid stresses, f body forces equal to $\rho \cdot g$ (g: gravitational acceleration), μ viscosity, ρ density and p pressure (R. Byron Bird 2006). For microfluidic devices where $N_{RE}<1$, inertial forces, thus, nonlinear terms, are negligible and viscous forces dominate fluid characteristics (Squires and Quake 2005). Hence, *Stokes Equation* can be written as;

$$\rho \left(\frac{\partial u}{\partial t} \right) = -\nabla p + \mu \nabla^2 u + f \qquad \textbf{(eq.2)}$$

For both of the cases mass conservation requires $\dfrac{\Delta \rho}{\Delta t} + \nabla \cdot (\rho u) = 0$.

Noting that, for incompressible Newtonian fluids with constant density $\nabla \cdot u = 0$.

Reynolds Number, N_{RE}, a generalized dimensionless mathematical expression to describe fluid flow characteristics is given by:

$$N_{RE} = \frac{l \cdot v \cdot \rho}{\mu} = \frac{F_{inertial}}{F_{viscous}} \qquad \textbf{(eq.3)}$$

where l is the characteristic length, v is linear velocity, ρ is density and μ is viscosity. Together in this form they represent the ratio of inertial forces over viscous forces.

When Reynolds Number is very low (<1), the flow is very predictable. The role of inertial forces in this phenomenon is explained by E.M. Purcell excellently in his speech in 1976 (Purcell January 1977) where he compares a human and a bacteria moving in water and the distance they move after removing the forces acting on the two bodies. The bacterium moves only 0.1Å due to the lack of inertial forces that would drag it, where human body establishes a decelerated motion for a longer while. Same analogy is valid for molecules flowing in a fluid. When no other forces are exerted, no significant inertial forces means no flow. When small forces are applied on the fluid and laminar flow is formed, fluid flows under the control of these forces and undisturbed by the inertial forces. Hence a very predictable, linear and neat laminar flow is formed (Beebe, Mensing et al. 2002).

Regularity of laminar flow is often utilized for some applications like microfabrication (Kenis 1999). When two immiscible fluids introduced into a microchannel without immersion or suspension, the interface between fluids creates a perfect line which is adjustable with flow velocity. This line created by means of laminar flow is a key point to produce a nano-wire created by precipitation reaction between two fluids. Another flow can be introduced into the channel again to remove the unnecessary parts by solving the precipitate or add another layer of the wire. High predictability of laminar flow is utilized in such applications for creating micro electrical circuits, sensors, separation of particles and even for fertilization purposes (Squires and Quake 2005, Swain, Lai et al. 2013).

Mixing or turbulent flow can often be very desirable. Especially in reaction systems, mixing is in paramount importance. Microfluidic devices are often used as micro-reactors for drug industries and for many fine chemical and biological processes (Dittrich and Manz 2006, Chiu 2007, Teh, Lin et al. 2008, Kuo and Chiu 2011). Special equipment or specially designed micro-channels are used to provide mixing for such operations (Beebe, Mensing et al. 2002, Jessamine M. K. Ng 2002, Stroock, Dertinger et al. 2002, Kuo and Chiu 2011). Another important aspect to be considered before wildly mixing substances is, separation of the substances to be sorted or analyzed later. Products of the reactions often needed to be separated and sadly, more you mix harder you separate (Squires and Quake 2005). Then, one should realize that mixing and dispersion issues are in great importance for microfluidic devices.

Mass transport mechanisms are explained by Fick's Law, which is in analogy of driving force over the resistance relation (Cui, Dykhuizen et al. 2002, Li 2006). When fluid flow is introduced into a diffusive system, continuity equation is often used to adapt the mathematical definitions into mass transfer system with fluid flow. The continuity equation and the steady and unsteady state forms of Fick's law are given by:

$$\textit{Continuity equation:} \qquad \frac{\partial \rho}{\partial t} + \nabla \cdot (\rho \mathbf{u}) = 0 \qquad \textbf{(eq.4)}$$

$$\textit{Fick's 1}^{st}\textit{ law:} \qquad J = -D \frac{\delta C}{\delta x} \qquad \textbf{(eq.5)}$$

$$\textit{Fick's 2}^{nd}\textit{ law:} \qquad \frac{\delta C}{\delta t} = D \frac{\delta C^2}{\delta x^2} \qquad \textbf{(eq.6)}$$

where, C is the concentration, u is the relative velocity, D is the diffusion coefficient, t is the time, J is the Flux and x is the distance.

Convective transport is the mass transport mechanism that is maintained by a bulk flow. Existence of velocity difference between fluid flow and a point which emits particles leads to formation of convective mass transport. Diffusive flux is the less dominant component of the mass transport and is maintained by the molecular motions. Diffusive flux always occurs no matter what material is the media or what physical state the media is in. Physical conditions only affect the rate of the diffusion. Convective mass transport only exists when a fluid flow is presented into the system. Fluid flow can be naturally occurring or may be a forced flow maintained by fans or other equipment (Geankoplis 2003).

A global method used to compare convective and diffusive mass transport is validation of Sherwood Number, a dimensionless number named in honor of Thomas Kilgore Sherwood. It is an important measure for comparison. It indicates the ratio of convective diffusion over molecular diffusion and is expressed as:

$$N_{sh} = \frac{k.L}{D} \qquad \textbf{(eq.7)}$$

where, k is the convective diffusion coefficient, L is the characteristic length in here 'radius of droplet' and D is the molecular diffusion coefficient.

The most important part of intracellular mass transport occurs at the cell membrane. Cell membrane is permeable to water molecules but it creates a resistive wall for CPA to diffuse. Cell membrane is not permeable to most CPA molecules like trehalose. However, glycerol is permeable to mammalian cell membrane (Palasz and Mapletoft 1996). In addition to mass transfer laws, mass transport through an organic membrane is defined by:

$$\frac{dN_s}{dt} = P_s.A(C_s^e - C_s^i) \qquad \text{(eq.8a)}$$

$$\frac{dV_w}{dt} = -L_P.A.R.T(\pi^e - \pi^i) \qquad \text{(eq.8b)}$$

Eq.8a and **eq.8b** are proposed by Jacobs M.H. in 1932-1933. Later another formalism including solute and solvent interactions (degree of interaction between solute and the solvent molecules defined by σ reflection coefficient) is proposed by Kedem-Katchalsky (Kedem and Katchalsky 1958) given by:

$$\frac{dV_{w+s}}{dt} = -L_p ART\left\{(C_n^e - C_n^i) + \sigma(C_s^e - C_s^i)\right\} \qquad \text{(eq.9a)}$$

$$\frac{dN_s}{dt} = (1-\sigma)\left(\frac{1}{2}\right)\left(C_s^e + C_s^i\right)\frac{dV_{w+s}}{dt} + P_s A\left(C_s^e - C_s^i\right) \qquad \text{(eq.9b)}$$

$$0 \leq \sigma \leq 1 - \frac{P_s v_s}{RTL_p} \qquad \text{(eq.9c)}$$

Equation.8a stands for solute transport across cell membrane and **equation.8b** represents water transport through cell membrane. In the above formalism definitions, Ns is solute amount, Ps is solute permeability (a coefficient specific to membrane), A is area, C is concentration, L_p is hydraulic conductivity (a coefficient specific to membrane), V_w is water volume, R is universal gas constant, T is temperature, σ is reflection coefficient and π is osmolarity. Superscripts e and i indicate extracellular and intracellular, respectively.

3. MATERIALS AND METHODS

3.1 Computing Platform

Hardware

All the computations were run on Hewlett Packard Z420 Workstation with Intel Xeon CPU at 3.20 GHz 8 cores 16 threads processor and 32 GB of random access memory (RAM). NVIDIA Quadro K2000 graphics card was integrated to workstation.

Software

64-Bit Microsoft Windows 7 operating system was used in the workstation. Comsol Multiphysics (Version 4.3) Finite Element Modeling software was used to create two and three dimensional models of the microfluidic system. Mathworks MATLAB (Version 2012b) and Microsoft Excel 2010 was used to support the calculations.

The main calculation software was Comsol Multiphysics. Transport of Diluted Species Module of Comsol is employed for the calculation of mass transfer. Laminar Flow module is employed for the calculations of fluid flow. Moving Mesh module is used to create the effect of shrinkage of aqueous droplets. MATLAB functions which compatibly work with Comsol are created for the detailed determination of fluid flow parameters such as relative velocity. Both MATLAB and Microsoft Excel software were used to create data fit curves from the resulting data which is imported from Comsol. Desired data is correlated by curve fits and definition function of the curve is exported back to Comsol for the sake of controllable and less sophisticated calculation sequence. Thin Diffusion Barrier node under Transport of Diluted Species Module is used to create the impact of cell membrane.

Our ultimate model we created was an 8000 micron long channel with fifteen droplets of 100 micron diameter carrying total three cells, and each droplet separated by 400 micron interval from droplet center to droplet center. Channel cross section was 150x200 microns and cells were 25 micron in diameter (see **figure-3.1**).
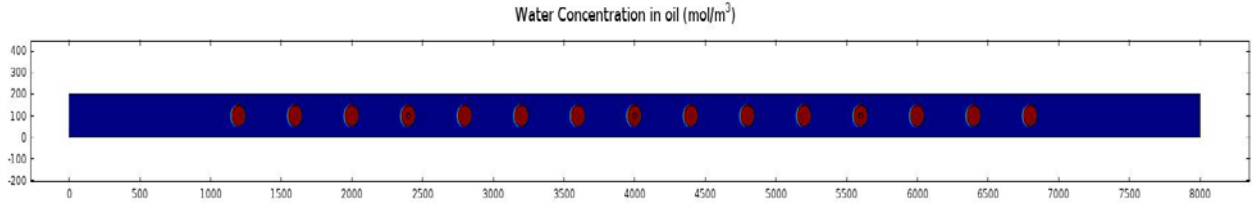
Figure.3.1- Appearance of the system at t=0.

Time dependent solver has used up to 300 seconds. Steps taken by solver were set to free mode, where backwards differentiation formula (BDF) method with maximum and minimum BDF order of 2 and 1 was employed.

Fully Coupled solver type is chosen for the sake of coupling of used physics in the model. Direct linear solver was used as the solver. To be able to conduct Multithreaded Solving (using 8 cores and 16 threads of the processor at the same time for different tasks when possible) Parallel Sparse Direct Solver (PARDISO) was chosen out of three types of Direct Solver. Nested Dissection Multithreaded algorithm is chosen for preordering. Two level scheduling method is chosen, which is a faster method when used with many processor cores. Multithreaded forward and backward solve option is used to improve performance by taking advantage of the processor cores.

Solving method was Newtonian Automatic Highly Nonlinear to achieve high convergence. Smallest allowed damping factor was 1×10^{-9} considering the micrometer dimensions of the system solved with metric system. Newtown Iterations were terminated by tolerance factor which was set to 0.01 with relative tolerance of 0.01.

3.2 Microfluidic System

Liquid organic phase was soybean oil, which is quasi-immiscible with water and has capability of solving water in small amounts (~0.4%) (He, Sun et al. 2004, Bajpayee, Edd et al. 2010). There are several suitable fatty alcohols that are capable of solving higher amounts of water. Soybean oil is chosen as the organic phase due to availability and low cost. Investigated favorable organic phases other than soybean oil were given in **appendix-7.1**. In experiments, surfactant was added to water droplets to render them form droplets easily in organic phase.

18

PDMS is an optically transparent soft elastomer with properties completely different than silicon. It supports use of pneumatic valves and provides ease of creation of the structure of microfluidic system. One disadvantage of PDMS is the mechanical or thermal reliability of the material. When necessary, glass, steel or silicon are useful materials to form rigid, thermally and chemically stable components. These materials are also useful in Nano-fluidics technology where channels need to be rigid (Mijatovic, Eijkel et al. 2005). On biological applications usually polymeric structure is preferred for manufacturing of microfluidic devices. They are easy to build by molding and transparent enough to allow use of optical methods of detection. Also PDMS is hydrophobic on surface, which is often advantageous for biological applications. The devices we studied are made of PDMS channel patterns bonded on glass slide, which creates three consecutive PDMS side and a glass side for rectangular micro-channels.

The manufacturing process for the polymeric micro-channels starts with visualization of 2-dimensional channel pattern drawn in computer aided design software (AutoCAD). This allows sensitivity through manufacturing process. In order to achieve the nanometer scale sensitivity, surface lithography is employed at the beginning of the process. The pattern drawn on CAD software is transferred on a silicon wafer by surface lithography. After this step, it is possible to produce a mold with the same height as the channel height. Mold is used as the negative replica of the channel pattern and 3-dimensional microchannel production can be started with casting the PDMS solution over the mold. Polymer solution is left to desiccation in a vacuum chamber to remove bubbles formed in the viscous polymer solution. Dried and bubble-free polymer is removed from the surface and the mold is taken out. At this step, three-sided rectangular micro-channel on the surface of PDMS is obtained. Finally, a glass slide and the PDMS are taken and put into oxygen plasma to make surface available to bond for PDMS. Polymer is put on the slide to bond in the way micro-channel will be left between the glass and the polymer. Result is a micro-channel with rectangular cross section available to monitor through glass side (see **Figure.3.2**).
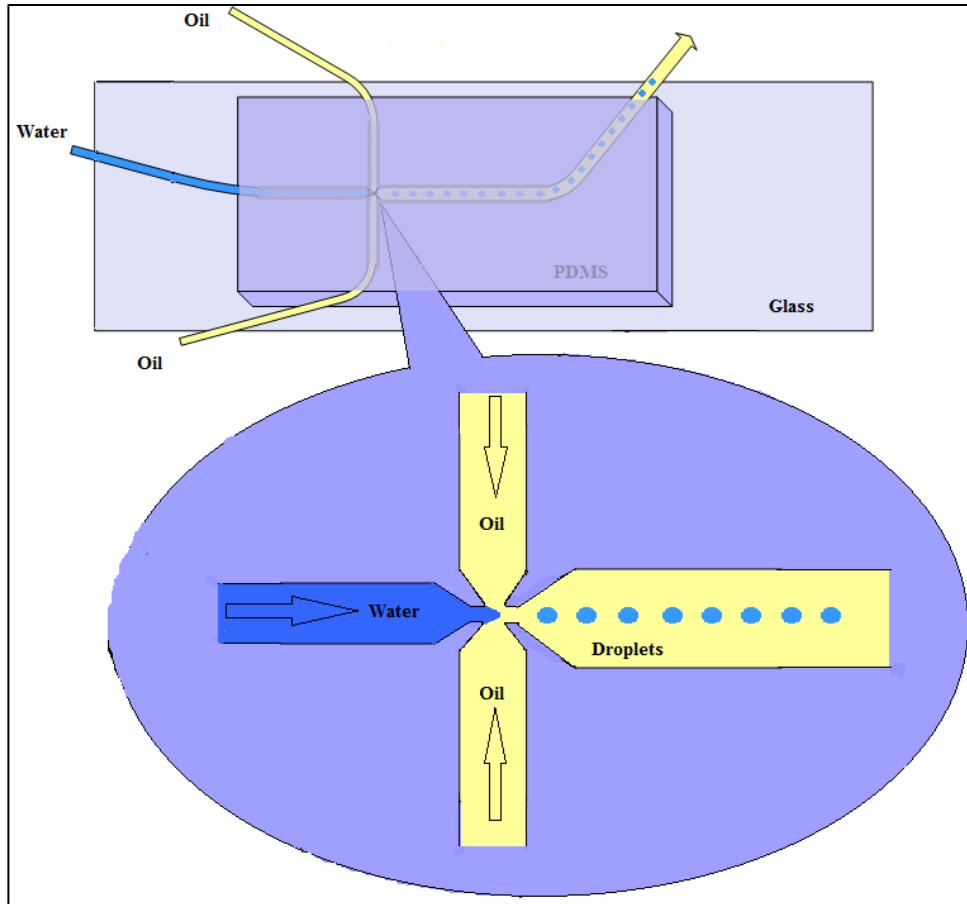
Figure.3.2- Microfluidic channel and the T-junction where droplets are generated.

3.3 Syringe Pump

In order to feed a microfluidic system one must have a very sensitive pumping system like peristaltic pumps or syringe pumps. Syringe pumps are systems that simply press a syringe very gently. The Nemesys syringe pump system with the microfluidic system was controlled with a software interface through pc. It was capable of pumping three syringes simultaneously and each flow rate can be adjusted separately from nanoliter to milliliter precision. Ends of the syringes were connected to microfluidic device as feeds. Connection tubings were polymeric tygon tubes with inner diameter of around 100 μm (see **figure-3.3**).
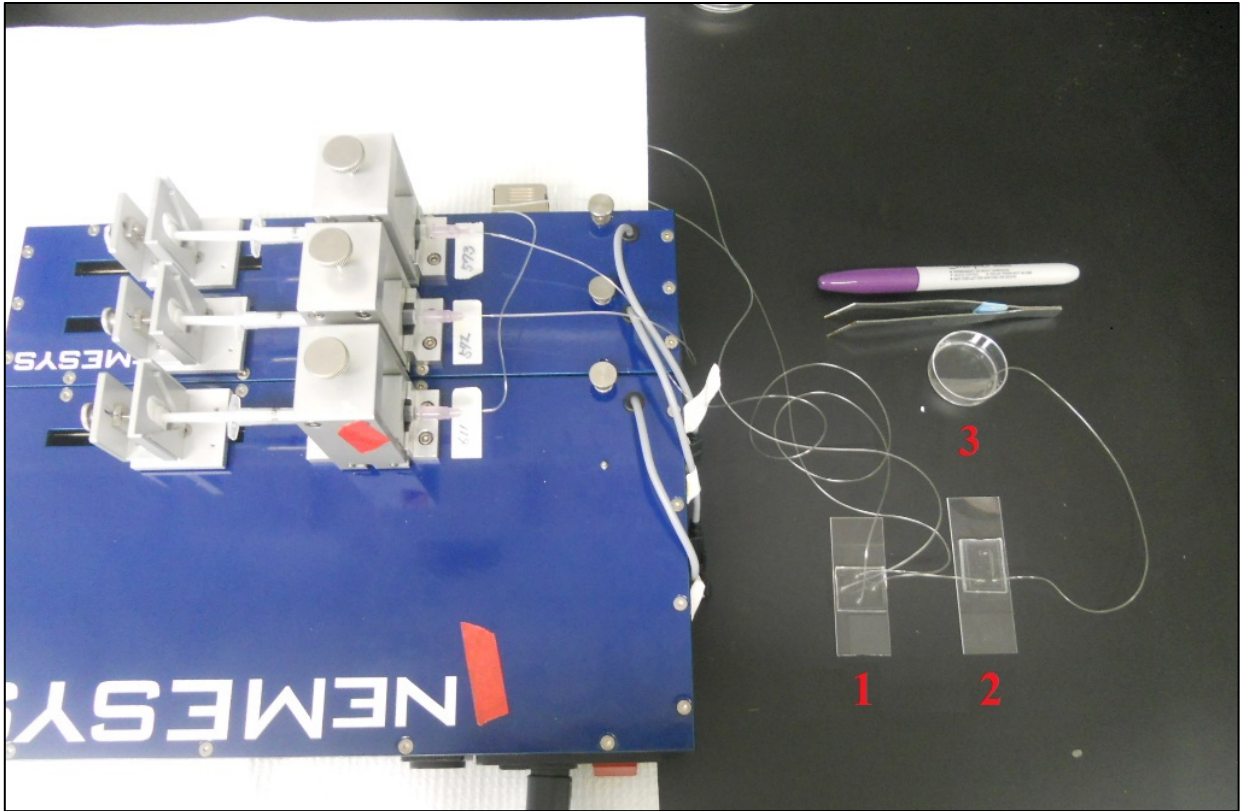
Figure.3.3- Syringe pump and a microfluidic setup developed by S. Onel at the Center for Engineering in Medicine and BioMEMS Resource Center. Numbers indicating order of flow from microfluidic devices to petri dish in the end.

3.4 Inverted microscope

We used an Axio Observer model fluorescent inverted microscope made by Carl Zeiss. It was an inverted microscope allowing us to monitor micro-channels from the underside through glass, free of the view disturbances caused by the fluid feed and PDMS on the upside of the microfluidic device. Microscope also had a user interface allowing us to observe through computer screen and save or analyze results (see **figure.3.4**). We were able to change flow rate using the syringe pump interface and see the resulting effects through the microscope interface on the same screen.
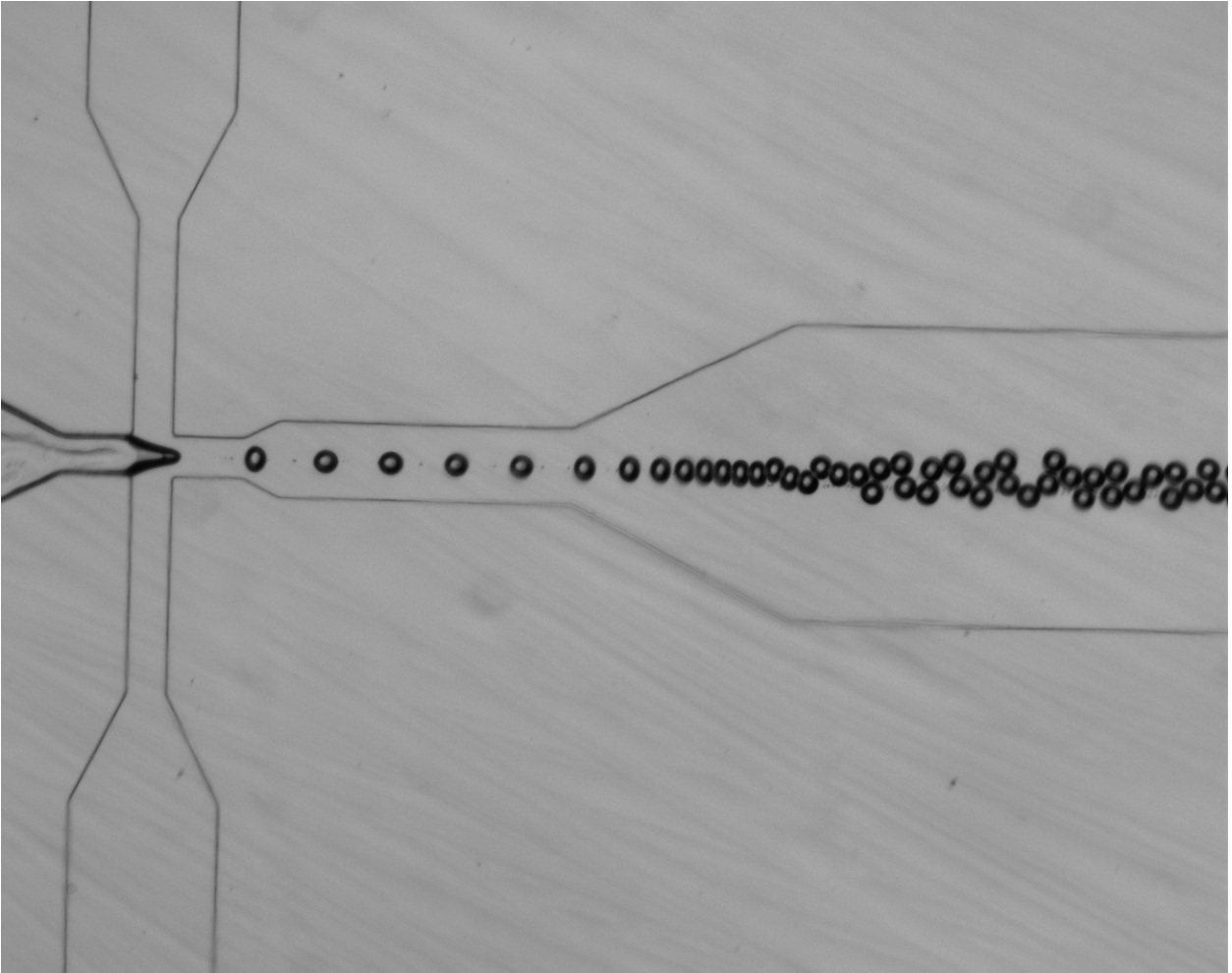
Figure.3.4 – A microscope image of pre-generated droplets. Droplets were generated by a T-junction.

3.5 ITO-Heaters

We used transparent heaters coated with Indium Tin Oxide (ITO) on one side. ITO cover over glass surface allows heating of glass rapidly when an external excitation is applied by DC voltage signals with certain wavelength absorbed by ITO layer. These heaters work with an analog controller system and a thermistor probe, which can maintain temperatures between 0-50 $^{\circ}$C. Heater is placed under the microfluidic device to heat through very thin glass without preventing any optical detection.

3.6 Calculations

3.6.1   System Definition

Figure-3.5 illustrates the system sections where we carried out calculations. We assumed that water diffuses freely through cell membrane with low resistance to diffusion, and that the water amount in the droplets is the sum of water present within the cell and water present out of the cell within the droplet.

Gradually increasing CPA concentration is the main purpose of the method which is tested in this thesis. Continuous increase needed in the CPA concentration is maintained by removal of water from the droplet. All calculations are performed for micro-channel with 150x200µm cross-section and flow regime was always laminar.
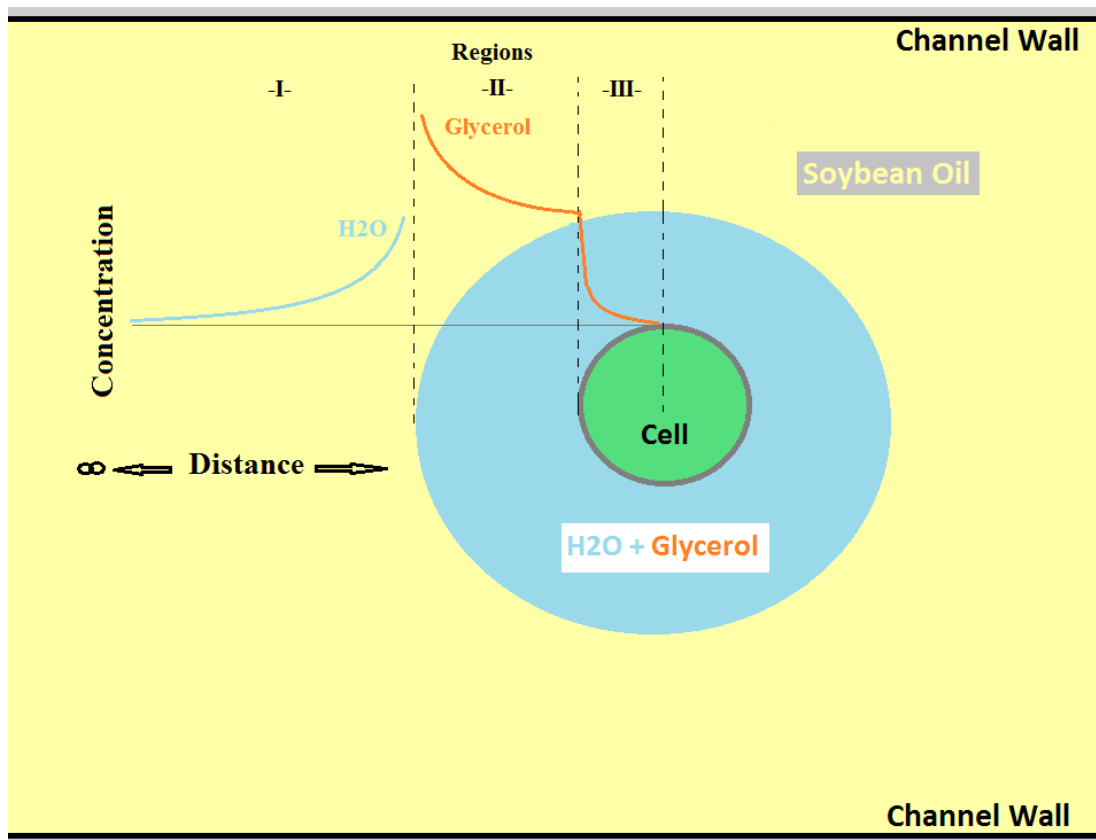

Figure-3.5. A representative figure of the regions that are modeled. Region-I- diffusion of water into organic phase, Region-II- Diffusion of CPA within droplet, Region-III- Diffusion of CPA through cell membrane and inner cell.

Organic phase which is saturated with water at initial operating temperature (20 °C) is introduced into the channel. Hence no net mass transport of water takes place at 20 °C. After producing desired droplet formation heat is supplied to system with an electronically controlled heater which can keep system at any temperature between 20 °C – 50 °C. As system is heated, solubility of water within the organic phase is enhanced, creating a concentration gap, a driving force, for water to diffuse into organic phase. Hence, a system is created where diffusion of water into organic phase is controlled by temperature.

Heat transfer resistance created by the microfluidic channel walls is neglected. Instant heat up from 20 C° to 45 C° assumption is made considering very small heat capacity of the fluids flowing in 150 µm x 200 µm cross section channel. Nevertheless, all the initial conditions and unsteady state mass and momentum transfer calculations are chosen or performed considering the temperature effects at 20 C° (lowest) and 45 C° (highest).

3.6.2 Mathematical Model

Calculation process was conducted in two steps, starting with the solving for concentration and water flux parameters in step-1. This very first stage of calculation is conducted using:

$$\frac{dC_i}{dt} = \nabla \cdot (D \cdot \nabla C_i) - u \cdot \nabla C_i + Rxn \qquad \textbf{(eq.10)}$$

$$J_i = -D \cdot \nabla C_i + u \cdot C_i \qquad \textbf{(eq.11)}$$

which are used with time dependent, direct solving sequence on Comsol software. C is concentration, u is relative velocity, D is diffusion coefficient, t is time, J is Flux, x is distance and Rxn is the rate of creation or destruction of chemical species. **Eq.10** and **eq.11** are derived from Fick's Law of Diffusion and Continuity Equation (**eq.4, eq.5** and **eq.6**) of conserved quantities to express convection and diffusion together.

It is shown on **eq.10** that flux value is directly proportional to relative velocity which is in fact the dominant factor that affects the flux. Increase in the relative velocity is the main reason for increase in water flux. One should not confuse volumetric flow rate with average linear

velocity. Total volumetric flow rate in the channel was 205 µl/s, which is equivalent of 683 µm/s linear velocity defined as U_{avg}.

In **eq.10 and 11,** terms including 'u' represent contribution of convective mass transport, terms including 'D' represent contribution of molecular transport and the term 'Rxn' represents reaction rate. There is no reaction in the system investigated. Hence, **equation.10** is used in the simplified form of convection-diffusion equation where Rxn=0. Relation between relative velocity and water flux is given in **eq.11.**

Relation between aqueous droplet radius and relative velocity is introduced separately via:

$$U_i = \left(R_i^2 - \frac{w^2}{4}\right) \cdot \frac{\Delta P}{L \cdot \mu \cdot 2} \qquad \textbf{(eq.12a)}$$

$$u = U_i - U_{avg} \qquad \textbf{(eq.12b)}$$

where, U_i is aqueous droplet velocity, r is radius or y-coordinate, w is width, P is pressure, L is channel length and μ is viscosity, U_{avg} is average organic phase velocity, u is relative velocity. **Eq.12 set** is calculated for U_i and u in separate software (Excel) and 'u' relative velocity is expressed as a function of 'R' droplet radius using curve fit tool of MATLAB.

Water flux and relative velocity can be defined as a function of droplet radius, leaving only time dependency of these parameters unknown. Time dependency of relative velocity can be expressed as a function of water flux given by:

$$\int_{R_i}^{R_0} V_i = \int_{R_i}^{R_0} J_i \cdot A_i \cdot t_i \qquad \textbf{(eq.13)}$$

where, V_i is volume of droplet, J_i is water flux into the organic phase, A_i is area and t_i is time. Noting that subscript i denotes time dependency.

Step-1 is completed by derivation of time and position dependent flux, aqueous droplet radius and relative velocity parameters. Results are used to start step-2, where calculations defining the inner part of the aqueous droplet are carried out (Region II and III on **figure-3.5**).

On the second step, change of CPA concentration within the droplet is calculated as a function of time and distance on Comsol. The first parameters used in step-2 are the time dependent

droplet volume and shrinkage rate of aqueous droplets which are leading to increase in concentration and are given by:

$$C_{i\_CPA} = C_{0\_CPA} \cdot \left(\frac{V_0}{V_i}\right) \qquad \text{(eq.14)}$$

$$\frac{dR_i}{dt} = U_{shrink} \qquad \text{(eq.15)}$$

where, C_{i_CPA} is CPA concentration at any time, C_{0_CPA} is initial CPA concentration and V_0 and V_i are initial and time dependent aqueous droplet volumes, respectively.

C_{i_CPA} value is used as the concentration value C_i and time dependent diffusion equation is given by:

$$\frac{dC_i}{dt} = \nabla \cdot (D \cdot \nabla C_i) \qquad \text{(eq.16)}$$

$$J_i = -D \cdot \nabla C_i \qquad \text{(eq.17)}$$

Comsol Multiphysics software uses **equations 16 and 17** when only diffusive flux is employed. These equations are simplified forms of **eq.10** and **eq.11** by the removal of convective terms and they depend on 'D' diffusion coefficient.

After solving for concentration of CPA in the droplet, **eq.8a and eq.8b** were introduced to system for calculation of mass transfer through cell membrane, which was necessary to determine ultimate result parameter **C_intracellular**, the concentration of CPA in the cell. **Eq.8a** and **eq.8b** are known as the Modern 2-Parameter Formalism in the literature, first proposed by Jacobs M.H. and D.R Stewart in 1932-1933 (Jacobs M. H. 1932, Jacobs 1933). (see end of **section 2.4**).

The mass transfer module in Comsol needs to be modified to model the diffusion through cell membrane described by **eq.8a,** which employs permeability coefficient 'P_s'. P_s needs to be converted to D using **eq.18** derived from **eq.11** and **eq.8a**;

$$-D = P_s . \Delta x \qquad \text{(eq.18)}$$

where, Δx represents the cell membrane thickness, Ps represents membrane permeability and D represents equivalent diffusion coefficient of the cell membrane.

COMSOL Moving Mesh module is used to represent the movement of the droplet walls during shrinking. There were also structural matters that should be considered while building the model. PDMS and glass channel surfaces have very smooth surfaces allowing fluids to flow without forming considerably thick immobile films over the walls. Average velocity value is used to define a slip velocity with ~10 percent of the average velocity and slip length of couple of microns for flow of the organic phase over channel surface.

On the final step all the data is gathered to find an optimum time, droplet size and average velocity to achieve the desired intracellular CPA concentration within mammalian cells via microfluidic devices. A flow chart of the aforementioned algorithm is given on **figure 3.6**.

Values of the constant parameters used in the calculations are given in **table-3.1.** Tables of parameters and variables used in Comsol simulations are given in **appendix 7.2**.

Table-3.1 – Constant parameters.

Parameter	Value	Reference
Water diffusion coefficient in Soybean oil (D_{wtr})	$0.5*10^{-10}\,m^2/s$	(He, Sun et al. 2004, Bajpayee, Edd et al. 2010)
Glycerol Diffusion coefficient in water	$0.825*10^{-9}\,m^2/s$	(Ternström, Sjöstrand et al. 1996)
(*) Cell membrane solute permeability (P_s)	$8*10^{-6}\,m/s$	(Yamaji, Valdez et al. 2006, Heo, Lee et al. 2011, Vian and Higgins 2014)
Cell membrane thickness	$8*10^{-9}\,m$	(Bruce Alberts 2008)
Viscosity of Soybean Oil (μ)	$0.058\,kg/m.s$	(Tong Wang 2005)

(*)Value may vary depending on type of the cell.

Given: C_i, C_f, R_0, U_{avg}, ΔP, L, w, μ, D_{wtr}

$U_{(i)}(t, R_i(J)), R_i(t, J_i(U))$

COMSOL

$$\frac{dC_i}{dt} = \nabla \cdot (D \cdot \nabla C_i) - u \cdot \nabla C_i$$

$$J_i = -D \cdot \nabla C_i + u \cdot C_i$$

B.C.1 : $x = R_i$, $C = C_f$
B.C.2 : $x = \infty$, $C = C_i$

LOOP

EXCEL or MATLAB

$$\int_{R_i}^{R_0} V_i = \int_{R_i}^{R_0} J_i \cdot A_i \cdot t_i$$

$$U_i = \left(R_i^2 - \frac{w^2}{4} \right) \cdot \frac{\Delta P}{L \cdot \mu \cdot 2}$$

$C_i(t,x), J_i(t,x)$

Step -1-

$V_i(R_i), A_i(R_i)$
$\Delta V(V_i, V_0)$
$C_{i\_CPA}(t_i, x, C_{0\_CPA})$

Given: $X_{membrane}$, $V_0(R_0)$, $A_0(R_0)$, C_{0_CPA}, $D_{glycrol}$

COMSOL

$$\frac{dC_i}{dt} = \nabla \cdot (D \cdot \nabla C_i)$$

$$J_i = -D \cdot \nabla C_i$$

$$\frac{dN_s}{dt} = P_s \cdot A \cdot \left(C_s^e - C_s^i \right)$$

$$-D = Ps.\Delta x \, , \, \frac{dR_i}{dt} = U_{shrink}$$

$C_{intracellular}$

Step -2-

Figure.3.6 – Algorithm generated to solve the system. C_i and C_f are saturated soybean oil concentrations at 20 C and 45 C respectively. R_0 is the initial droplet radius, U_{avg} is the average flow velocity of the organic phase, ΔP is the pressure difference exerted to maintain flow, L is the channel length, w is the channel width, μ is the oil viscosity, D_{wtr} is the diffusion coefficient of water in soybean oil, $X_{membrane}$ is the thickness of the cell membrane, V_0-A_0 are the initial volume and area of the droplet, C_{0_CPA} is the initial CPA concentration in the droplet, $D_{glycerol}$ is the diffusivity of glycerol in water and P_s is the solute permeability of cell membrane. u is the relative velocity between oil and droplet, U_i is the velocity of the aqueous droplets, R is the droplet radius, C is concentration, J is flux, N is mass, t is time, x is distance. Calculations of step-1 with the Loop represents calculations for outer droplet, calculations of step-2 represent the inner droplet. Subscript 'i' denotes time dependent (anytime), '0' denotes initial, 's' denotes solute, 'shrink' denotes shrinkage. Superscript 'e' denotes extracellular, 'i' denotes intracellular. $C_{intracellular}$ is the ultimate result of the calculations which represents CPA concentration within the cell at any time.

4. RESULTS AND DISCUSSIONS

4.1 Two Phase Flow in Micro-channel / Design Matters

Mass transfer and momentum transfer in this system cannot be considered separately because, fluid velocity enhances convective mass transport and as the mass transport takes place, droplets shrink and accelerate. Hence, mass transport instantaneously enhances droplet flow velocity. Diffusion is wanted to be hold at its maximum value, while temperature is employed to control the diffusion rate. However, in a microchannel, the absolute flow character is laminar flow, which does not allow mass transport to be kept in its maximum possible value. Higher mass transport rate can be achieved by utilizing convective mass transport which is only possible with creation of velocity difference between substances.

The important aspect to be focused on regarding convective mass transfer is the fluid-fluid interface region, which is the region where two fluids flow side by side with a velocity difference and create a potential for convective transport of the species. The originality of this research is owing to the outcomes of velocity difference between the droplets and average organic phase flow velocity. That is a required condition to apply convection-diffusion equation for mass transport on a system. Also, according to continuity equation, average velocity of the bulk fluid should be taken into account in order to calculate amount of mass transferred. Average velocity of the organic phase (bulk flow) does not change in the process.

Flow velocity profiles and the position of droplet in the profile were given on **figure-4.1**. That is a conventional laminar flow profile appearance for any Newtonian fluid forced to flow by pressure and flowing up to N_{RE} value of 2000. No matter what velocity the fluid is flowing at, the position on y-coordinate where the fluid hits the average velocity is the same (position of the orange line in y-direction on **figure-4.1**). The y-coordinate value, where the fluid flows at the speed equal to the average velocity does not change. This average velocity region, so entitled $R_{critical}$ region, is only a factor of channel width, not flow rate. The relative velocity value of our system hits to zero at that critical point, resulting a lower peak of flux magnitude of water into organic phase (see **figure.4.2**).
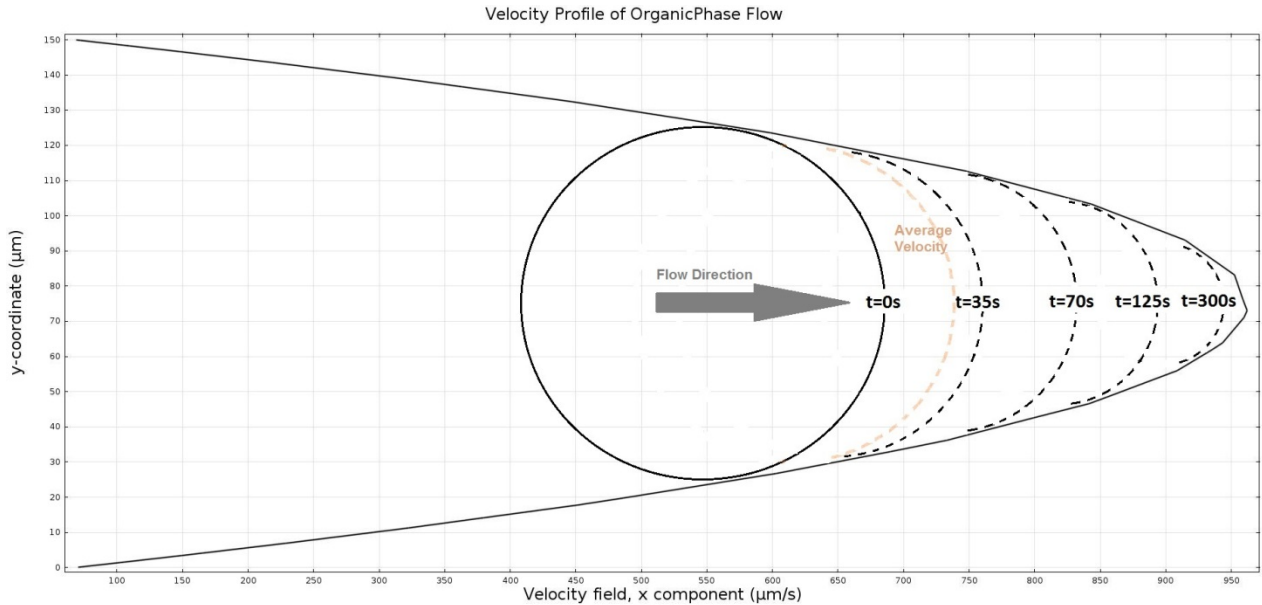
Figure.4.1 – A 100 micron droplet position shown on the velocity profile of the organic phase at 683µm/s flow rate. As the aqueous droplet shrinks, it is dragged into faster regions of the velocity profile. Dashed lines are visionary droplets at mentioned times. Orange line represents average velocity.

One can observe in **figure-4.1** that as the droplet size decreases, droplets are dragged into the faster regions of the fluid flow profile. Thus, the velocity difference between the droplets and the average organic phase flow velocity changes through time. A large droplet with $R>R_{critical}$ at the beginning, flows slower than the average organic phase velocity. As water diffuses into the organic phase and the droplet shrinks, it enhances its pace. First it reaches the flow speed of the average organic phase at $R=R_{critical}$, where only diffusive mass transfer takes place, and then keeps accelerating until water diffusion is ceased at an equilibrium state of concentration where $R<R_{critical}$. Mass transport rate of water drops dramatically in the $R=R_{critical}$ state, until droplet velocity passed average organic phase flow speed. In this thesis, this retarded mass transfer state is entitled Critical Radius State and the Radius in that interval is entitled as $R_{critical}$. For N_{RE} is less than 1, with laminar flow in the channel, the droplet will always be positioned in the center of the channel width (y-axis). The flow profile seen on **figure.4.1** is based on **eq.12a** derived from equation of motion (R. Byron Bird 2006).

Change in the radius causes change in relative aqueous droplet velocity which affects flux magnitude as seen in **figure-4.2**. Flux value is lowest at $R\sim=45$ and is valid for all flow rates

since the $R_{critical}$ value is only proportional to channel width. The proportionality value can be found on slope of **figure-4.3.**
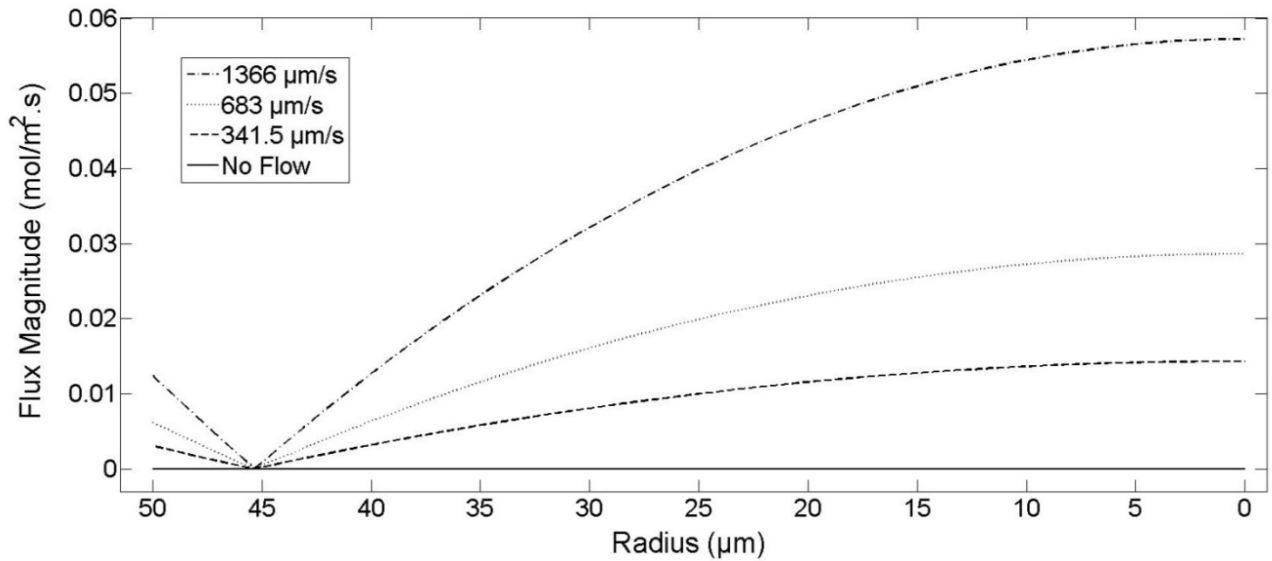

Figure-4.2. Change of flux magnitude with respect to droplet radius for various average organic phase flow rates.

Below $R_{critical}$ value, as the droplet radius decreases, flux continues to increase due to increase in relative velocity of aqueous droplets. This increment is proportional to the flow velocity magnitude of the organic phase.

At Rcritical, where relative droplet flow velocity is close to or equal to zero, no convective flow is utilized and a decreased droplet shrinkage rate is achieved. Flux magnitude hits the minimum value which roughly is equal to diffusive flux magnitude.

Figure-4.3 shows the Rcritical values that should be avoided at various channel width values. For example; if droplet size is 150 micron (R =75 micron), one should choose channel width of 250 microns or higher to avoid R critical region.
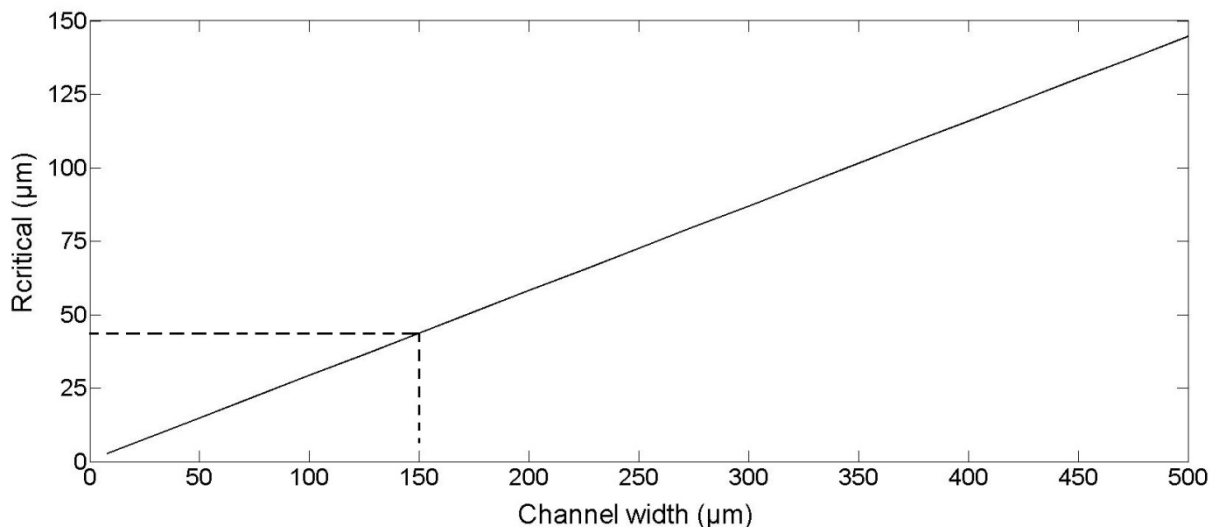
Figure-4.3. Critical Radius value for various channel width values. Equation of the line is **y=0.3028x**. Dashed line represents the $R_{critical}$ value for 150x200 microns cross sectioned channel in our work.

4.2   Transport of Species

Mass transport, is the most important agent in this research. All the other means of transport of matter and energy is used to enhance or keep the mass transport of the species under control within the channels. The concentration has always been the weightiest parameter in all the calculations and considerations.

Mass transport within the droplet and out of the droplet was handled separately, since they have distinct divergences. On **Figure-3.5,** our system is separated into three regions for ease of understanding. Also mobile and immobile phase assumption is exerted to reduce the complexity of the calculations. Considering the relative positions of the phases with respect to time, water can be addressed as the mobile substance in organic phase surrounding the droplet, which is presented as region-I- on **Figure-3.5**. Within the droplet (region-II- and -III- on **figure.3.5**), CPA can be addressed as the mobile substance diffusing through water and cell membrane, but not diffusing into organic phase. The mutual effect of two mass transport actions on each other in two different regions (inner and outer droplet) is constructed through

amount of water present in the droplet. By migration of water from the aqueous droplet surface into the organic phase, water amount in the aqueous droplet decreases continuously. Since definition of concentration is the ratio of mass content to volume of solution, decrease in the solution volume leads to an increase in the concentration. Computer aided iterative calculations are performed to solve aforementioned relations numerically.

4.2.1 Transport of Water from Aqueous Droplet to Organic Phase

At zero flow rate only diffusive mass transport takes place. In any magnitude of flow rate larger than 0, convective and diffusive mass transport takes place simultaneously. Increasing average flow velocity increases relative velocity magnitude, which creates a bigger convective mass transport potential. Droplets shrink the fastest at the highest flow rate (see **figure.4-4**).
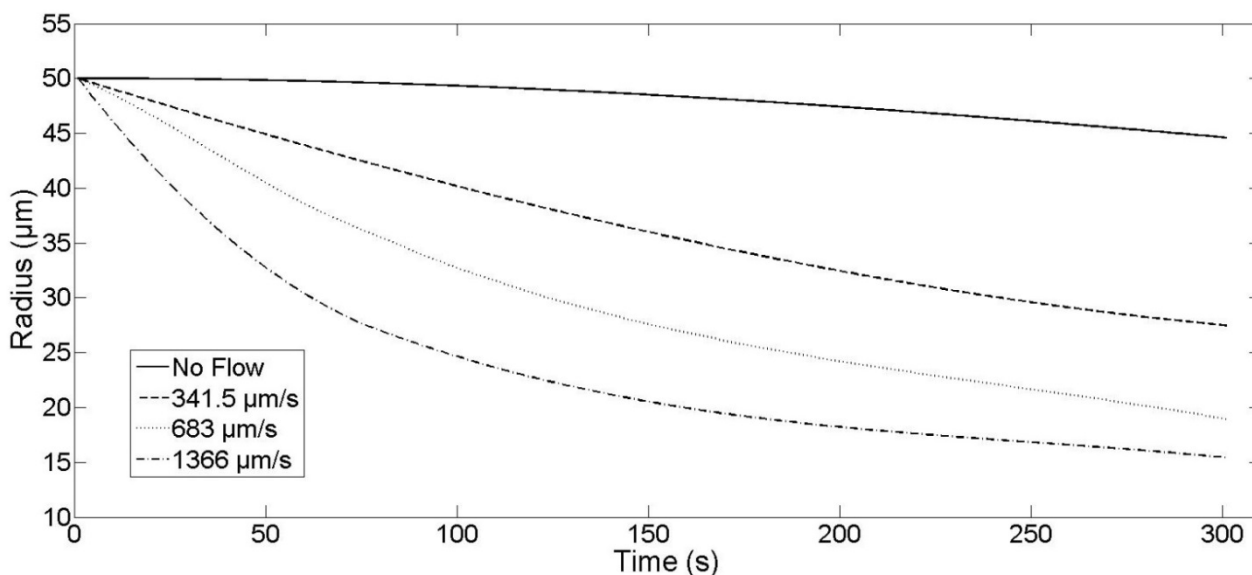
Figure-4.4. Radius of aqueous droplet with respect to time at various flow rates.

Aqueous droplet velocity relative to average organic phase flow velocity is defined as relative velocity. When relative velocity value is zero, droplets are flowing at average bulk phase velocity. This state develops at the instant, when droplets reach the critical radius at R=45μm. When relative velocity is zero, convective mass transport is at the minimum value (see. **Eq.10**

34

and eq.11). The relative velocity is analyzed since it is the dominant factor that effects convective diffusion (see **figure.4-5**).
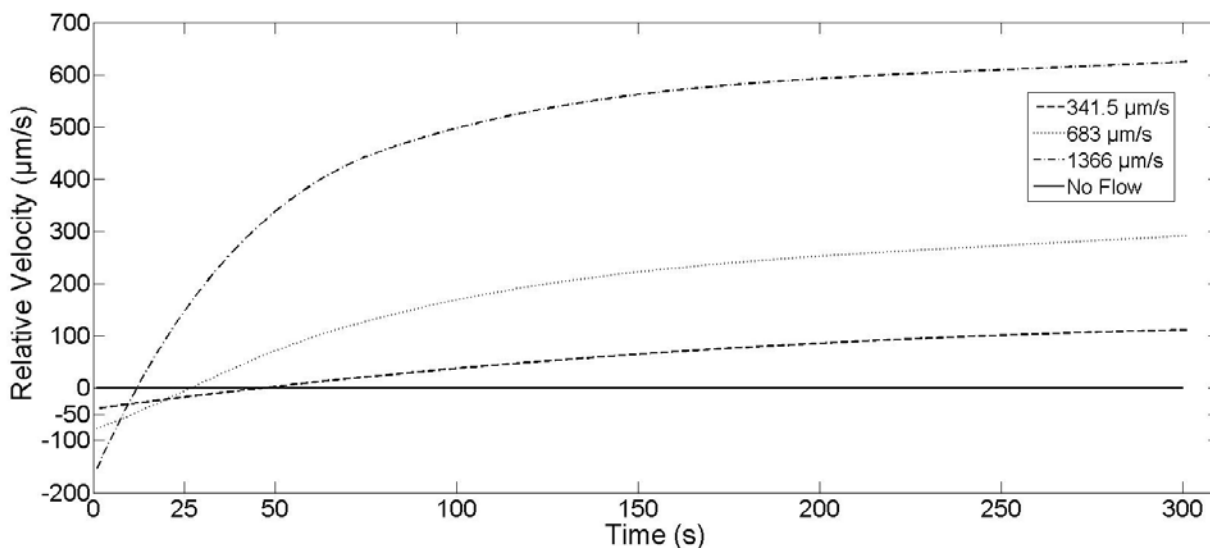
Figure-4.5. Difference between the velocity of aqueous droplets and average organic phase velocity with respect to time.

Total flux magnitude is the sum of convective flux magnitude and diffusive flux magnitude. At the instant droplet velocity catches average bulk flow velocity (zero relative velocity), flux values hit a lower peak point, where the flux value is nearly equal to the diffusive flux magnitude or nearly equal to the flux magnitude of No Flow case. Increasing the flow rate leads to achieving higher water mass flux from water to organic phase. **Figure-4.6** shows the total flux magnitude of water transport from droplet to organic phase.
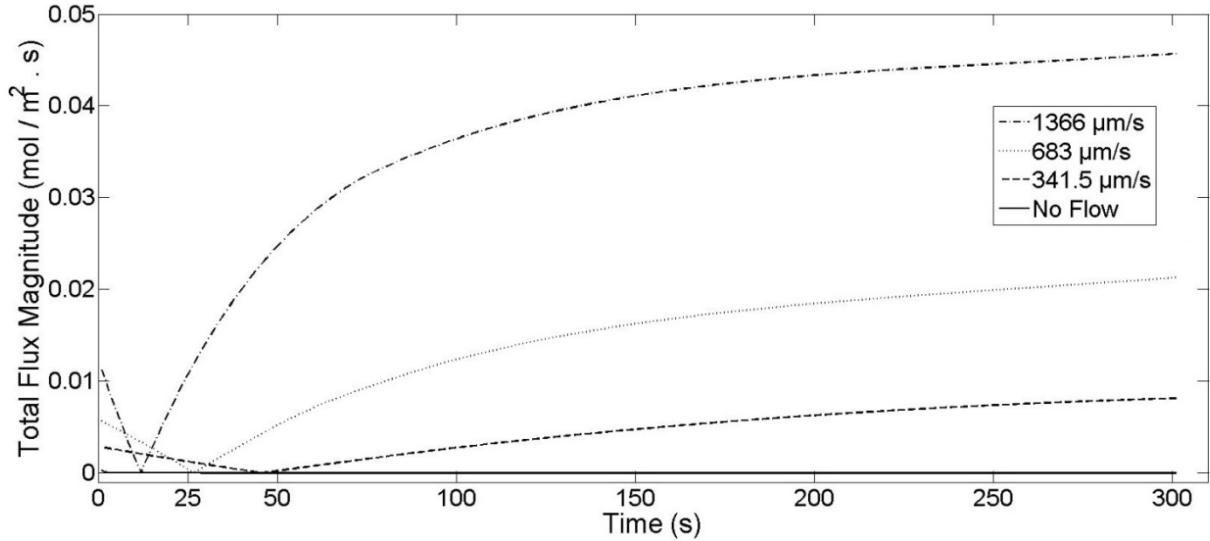
Figure-4.6. Total flux magnitude with respect to time at various flow rates.

Flux magnitude is always increasing after $R_{critical}$ region. Surface area of the droplet, where the mass transfer takes place, decreases in time. Hence a decrease in the mass transfer rate occurs when decrease in the area become dominant. **Figure-4.7** shows a combination of the results shown in **figure-4.4** and **figure-4.6,** where the flux magnitude value is represented in moles/second basis instead of moles/area·second basis. A decrease in total mass transfer develops due to reduction of area of the shrinking droplets**.** According to **Figure-4.7**, 1366 µm/s flow rate line is already at its maximum rate, while 341.5 µm/s flow rate is at the lowest. This indicates the importance of the flow rate for avoiding inhibiting effects of $R_{critical}$ region and for increasing convective mass transfer.
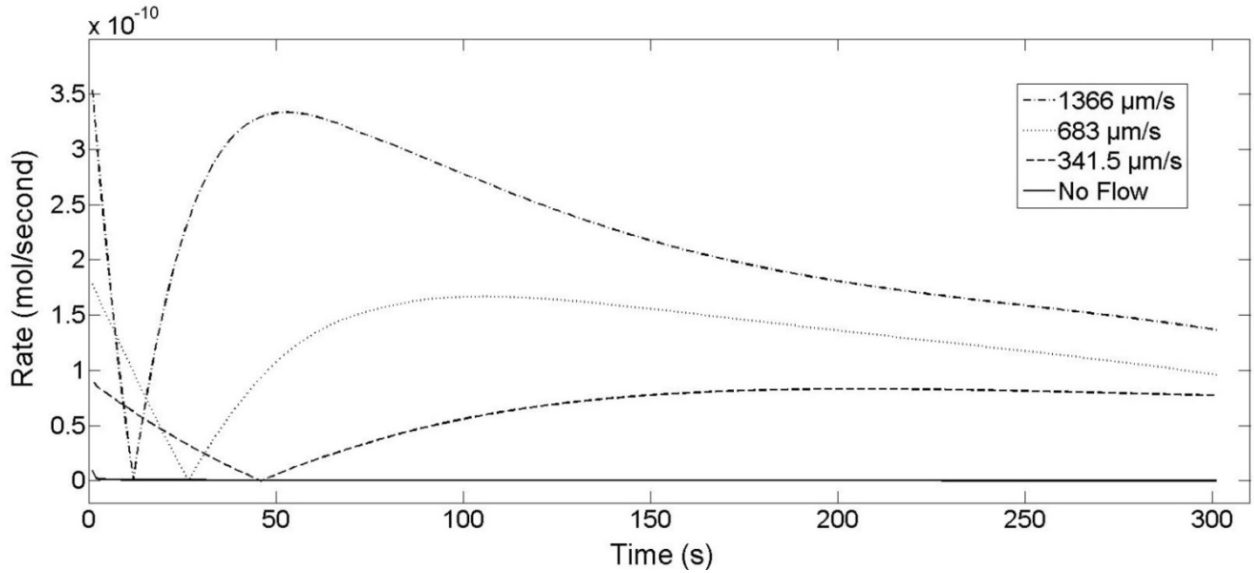
Figure-4.7. Transfer rate of water into organic phase with respect to time.

Higher flow rates provide better diffusion of water into the oil compared to the 'No flow' condition, where the flux value is the lowest. At low flow rates, concentration profiles within the channel wall stay close to those of the No Flow condition up to several minutes. That is a result of low relative droplet velocity values around the Rcritical region. Change in the direction of relative velocity retards the removal of water from the aqueous droplet. Droplets flowing in low bulk flow velocity reach R critical region the latest and, they stay in that region longer than higher flow rates due to the low shrinkage rate of the droplets. At low flow rates convective diffusion is not sufficient for droplets to shrink quickly and get off the R critical region. In **figure-4.8D,** only after t=120s, droplets in 341µm/s flow rate manage to set a less complicated flow regime and more predictable concentration profile (see **figure-4.9**). This reduced flux occasion is valid for all flow rates (1366µm/s flow line on **figure-4.8A** and 683µm/s line on **figure-4.8B**) but faster the flow rate shorter the time spent in the retarded flow region.
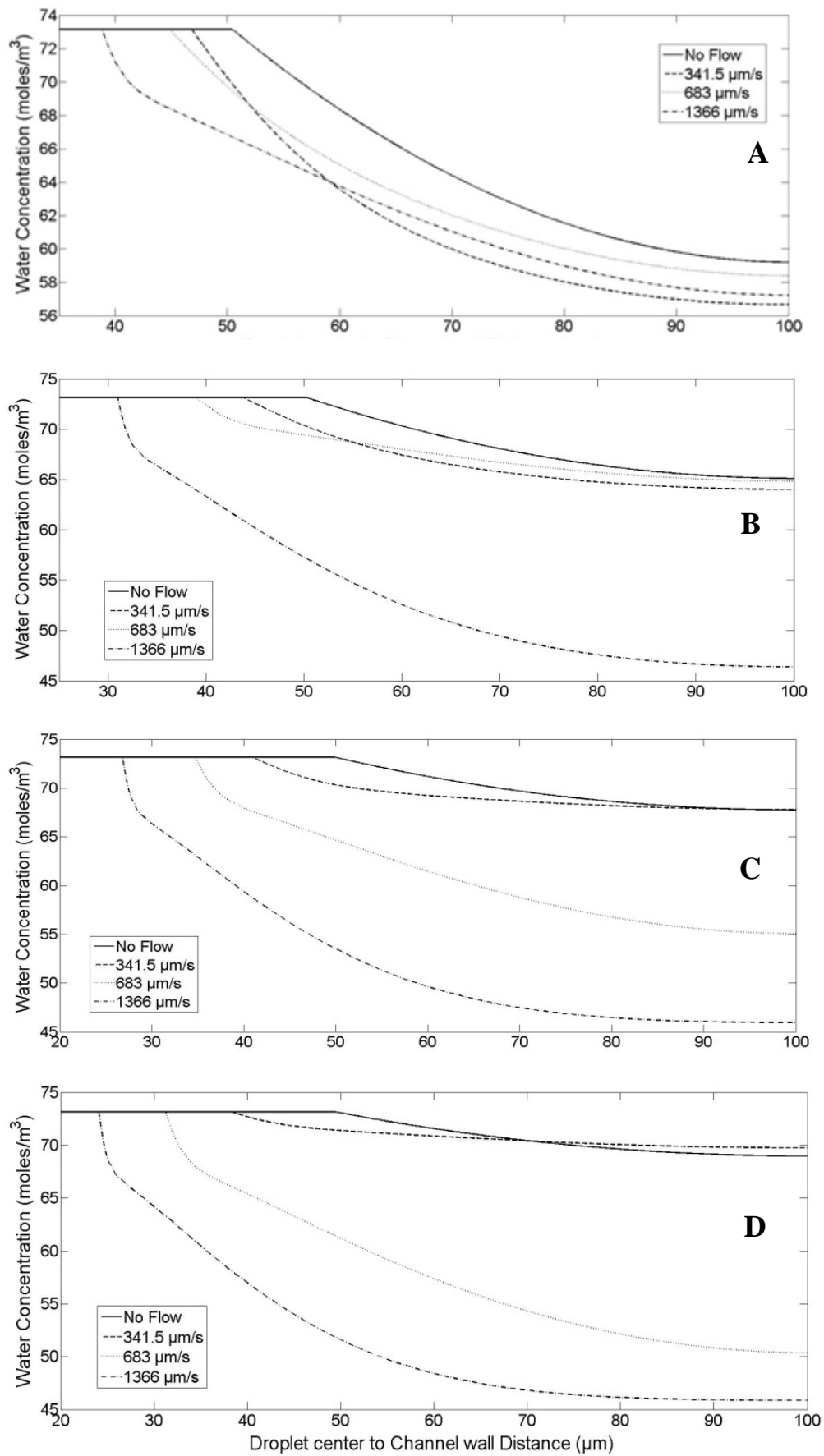
Figure-4.8. Concentration profiles of water in the organic phase for various flow rates with respect to position between droplet and channel wall at (a) t=30s, (b) t=60s, (c) t=90s, (d) t=120s.

In **figure-4.8D**, all the profiles of water concentration represent region-I- area on **figure-3.5** and, water concentration values stay same within the droplet equal to saturated water concentration in oil at 45°C.

Concentration profiles at high flow rates are more steady than lower flow rates. During the shrinkage of the droplets, when they pass through $R_{critical}$ region, practically a mixing occurs in the channel. During the process, flow direction does not change, but relative flow direction does change. At 341µm/s flow rate and at t=30, average organic phase velocity is faster than that of the droplet velocity. At t~=50 s, droplet radius value is equal to $R_{critical}$ value and the flow rate of droplet and average organic phase is equal. At t=60 s, droplets are shrunk and flow faster than average organic phase flow velocity. Water molecules dragged away from one droplet are now dragging back to the same droplet causing an affect similar to mixing instead of dragging away. As a result of low concentration gradient the water mass transport to organic phase slows down. At t=120 s, all the water molecules are dragged far away and a concentration profile of a conventional two phase flow is formed and continued steadily. At 683 and 1366 µm/s flow rates, droplets have already shrunk enough to flow faster than average organic phase velocity at t=30 s. The main advantage of faster flow rates is that the droplets come into contact with higher amounts of fresh organic phase that is less concentrated with water and has better capability of carrying away water molecules. Higher droplet velocity relative to average organic phase yields better mass flux. An image matrix describing water concentration in organic phase for different flow rates is given in **figure-4.9**.
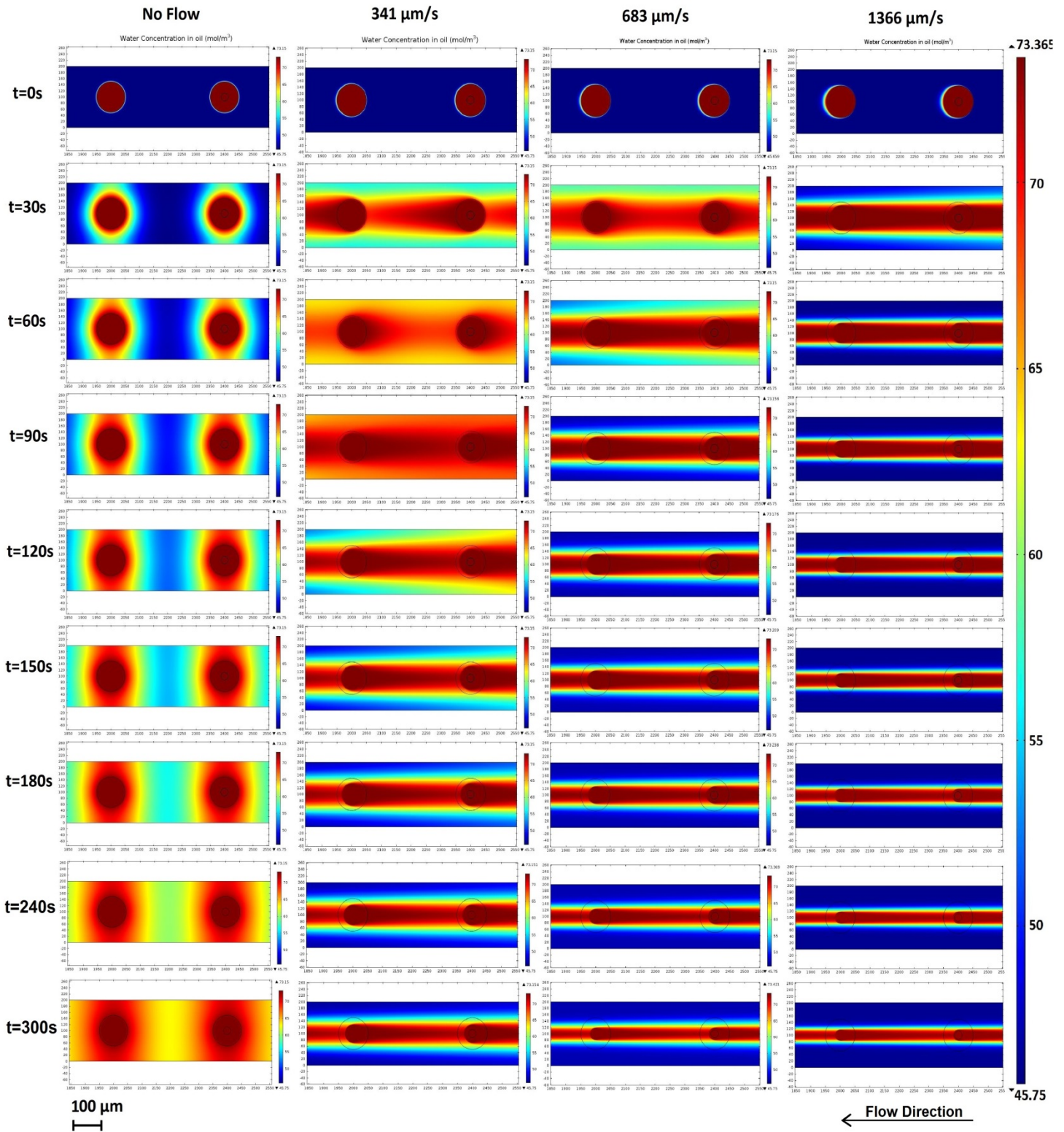
Figure-4.9. Concentration of water (mol/m^3) in organic phase for various flow rates at various times. Initial droplet diameter is 100 microns and channel width is 200 microns.

Local convective transport of water into the organic phase is effective, but diffusion of water from aqueous droplet to channel walls, perpendicular to flow direction, through the organic phase, will be as slow as molecular diffusion due to laminar flow (see **eq.10** and **eq.11**). Convective effects will not be perceivable for transport of water through the organic phase where net bulk flow velocity of water molecules in the organic phase is zero. That is why one should be sure that sufficient amount of organic phase is presented into the micro-channel to keep diffusion of water through organic phase at a reasonable level by keeping concentration gradient high and remove water from the aqueous droplets efficiently. Mentioned less active mass transport is sometimes helpful because if it was too fast, the concentration would be increased so fast and the cell might get damaged due to sudden osmotic pressure increase. For droplets larger than 0.5µm and glycerol concentration up to 6M, diffusion rate of water within the aqueous droplet is much higher than the diffusion rate of water through the organic phase (Bajpayee, Edd et al. 2010). This indicates that the transport of water through the organic phase is the limiting factor in our system and our operating range. Even if the temperature is increased suddenly, response of the organic phase to temperature adjustments would be slow which prevents osmotic pressure injury on cells.

4.2.2   Transport of CPA within Droplet

Mass transport mechanism within the droplet is considered to be molecular diffusion only. Circular flow motions within the cells caused by interfacial frictions at the droplet surface are not considered, since their effect on the total CPA concentration is insignificant. Also, water diffusion within the droplet is always faster than it is in organic phase (Bajpayee, Edd et al. 2010).

Degree of interaction in the membrane channels between permeating solute molecules and water molecules is defined as Reflection coefficient defined by Kedem-Katchalsky (Kedem and Katchalsky 1958, Kedem 1961) (see **eq.9**), from the previous work of Staverman in 1952 (Staverman 1952), where he defined reflection coefficient as the solute selectivity of the cell membrane. For dilute solutions, it is tested by Kleinhans (Kleinhans 1998) that the reflection coefficient is yielding same results with two-parameter formalism which does not include

reflection coefficient. For non-dilute solutions, reflection coefficient presenting a minor (~%5 volume change of cells at 10M) deviation and it is indicated that 2-parameter formalism is still a good approximation (see **figure-4.10**). Since we are testing concentrations up to 6M and inclusion of reflection coefficient is increasing the complexness of the model, we chose to carry on our calculations using modern two-parameter formalism which is commonly used today to describe cellular osmotic response of the cells to concentration changes (Elmoazzen, Elliott et al. 2009).
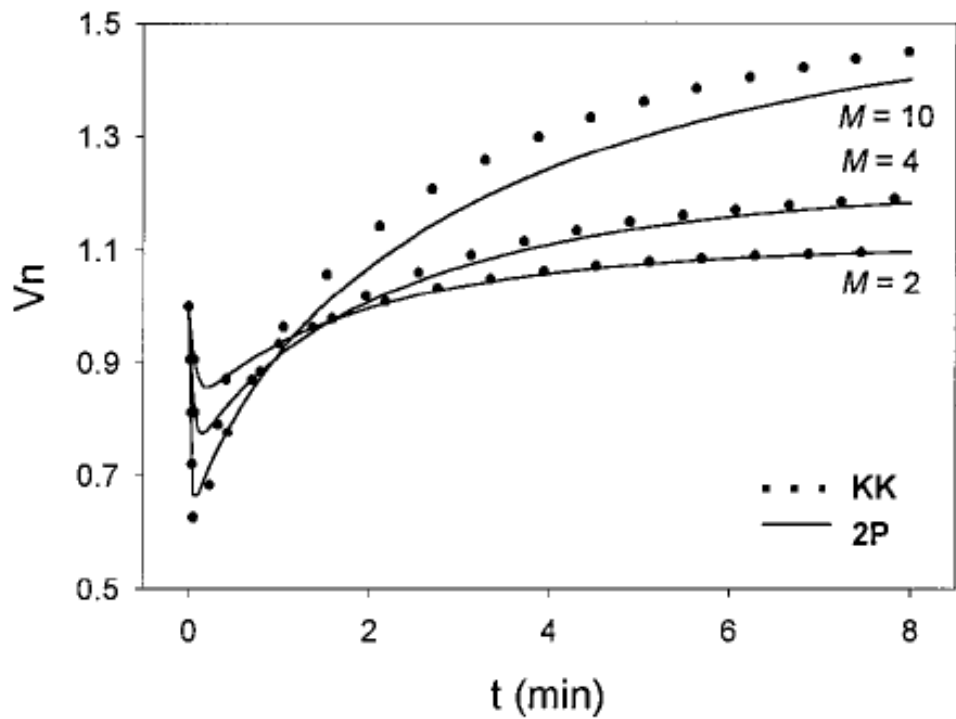
Figure-4.10. Comparison of cell response with Kedem-Katchalsky method and 2-Parameter formalism by Kleinhans (Kleinhans 1998) for different glycerol concentrations indicated by molarity (M).

43
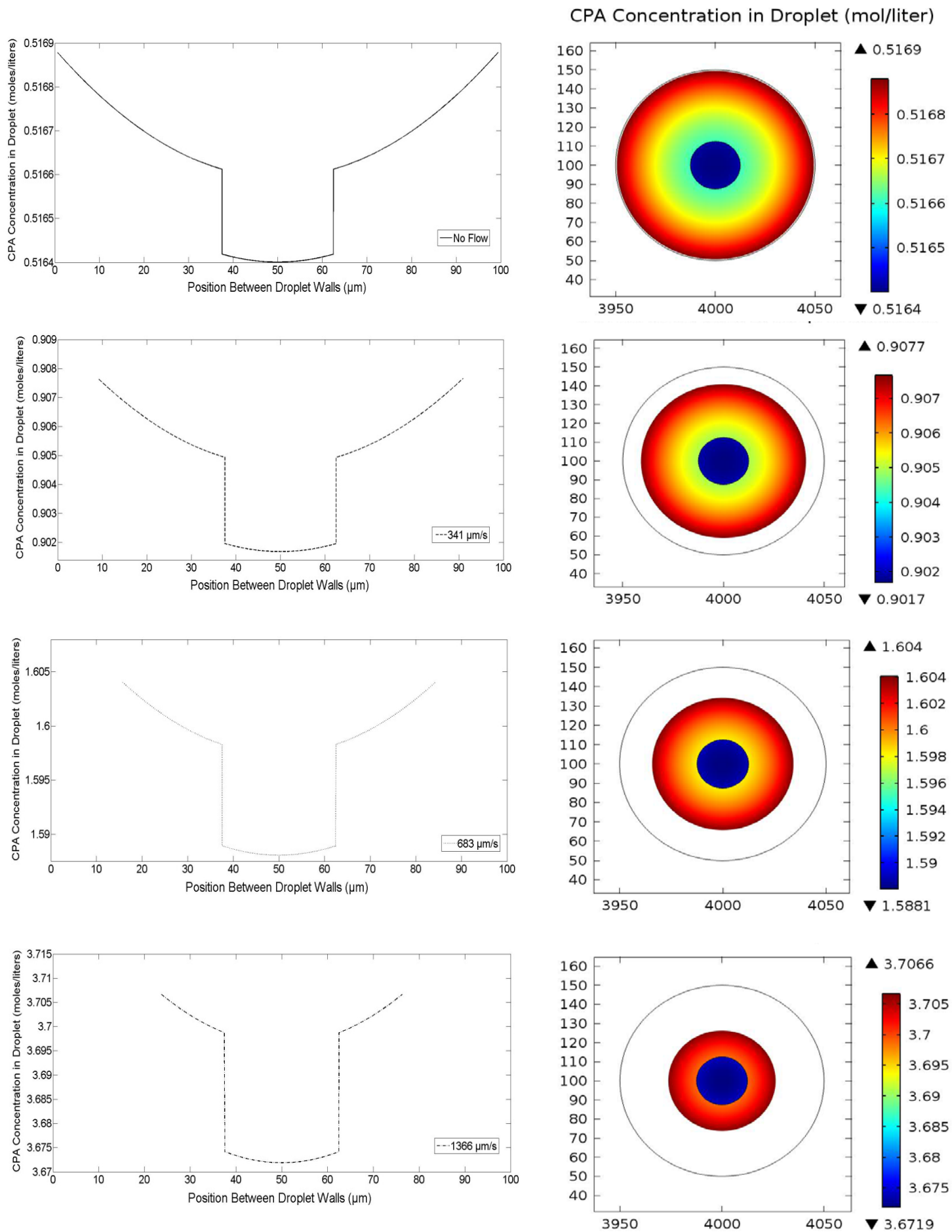
Figure.4.11 - CPA concentrations within the droplet for various flow rates at t=90s. All concentrations are in mol/liter. Initial concentration is 0.5M.

Figure-4.11 represents region-II- and -III- shown on **figure-3.5**. Concentration within the droplet is highest at droplet walls since the loss of water takes place at droplet walls in contact with the organic phase. Sudden decrease in CPA concentration is due to resistance of cell membrane against diffusion. Permeability of the cell membrane is used as Ps=8*10^{-6} m/s.
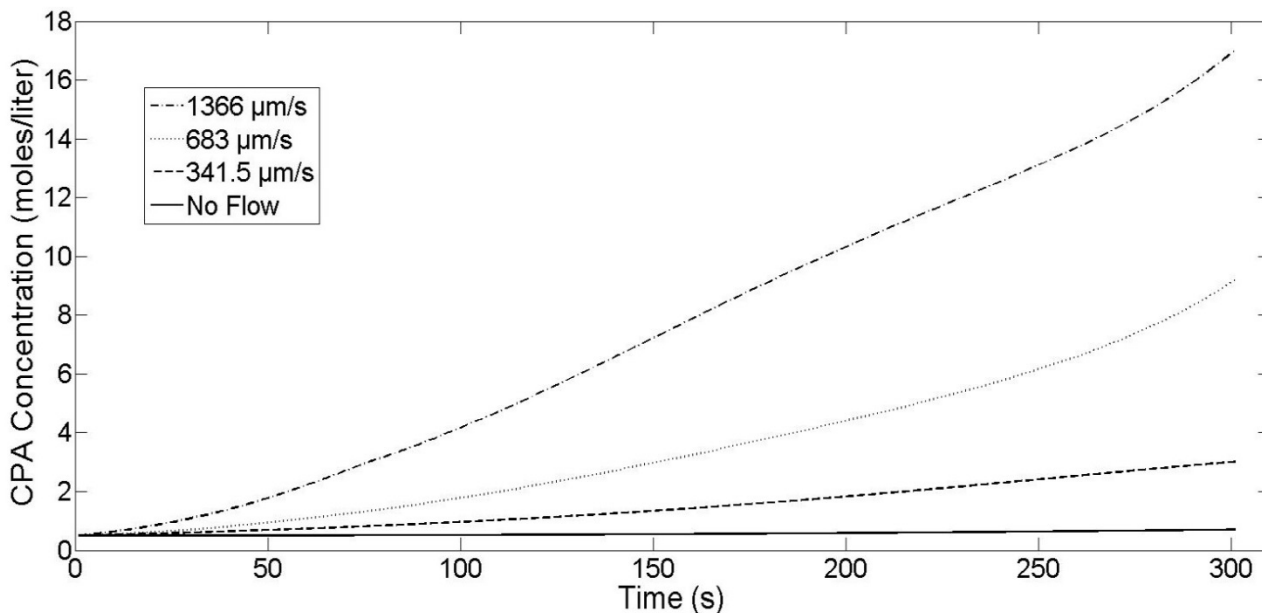
Figure-4.12. Change of CPA concentration within aqueous droplet due to shrinkage at various flow rates with respect to time. Initial CPA concentration is 0.5M.

As higher amounts of water is transported to organic phase with time, less amount of water is remained within the aqueous droplet increasing the concentration of CPA in the droplet as shown in **figure-4.12**. Faster shrinkage rate is achieved at higher flow rates yielding higher CPA concentration values.

4.3 Comparison of Convective and Conductive Water Transport in the Channel

Convective diffusion is in great importance compared to molecular diffusion, and it is the dominant component of overall mass transport. We take advantage of convective mass transport to promote overall diffusion of water into the organic phase. Local convective mass transport takes place over the droplet surface within the liquid-liquid interface. Although organic phase flow is laminar, the liquid-liquid interface, where two liquids are flowing with different velocities, provides satisfactory flow condition that is required for convective mass transport to be formed.

Figure-4.13 indicates the dominance of convective diffusion over molecular diffusion at 341.5μm/s, 683μm/s and 1366μm/s flow rate. At R critical, where velocity difference between droplet and average oil velocity is zero Sherwood number peaks to lowest point. Sherwood number is given by **eq.7**.
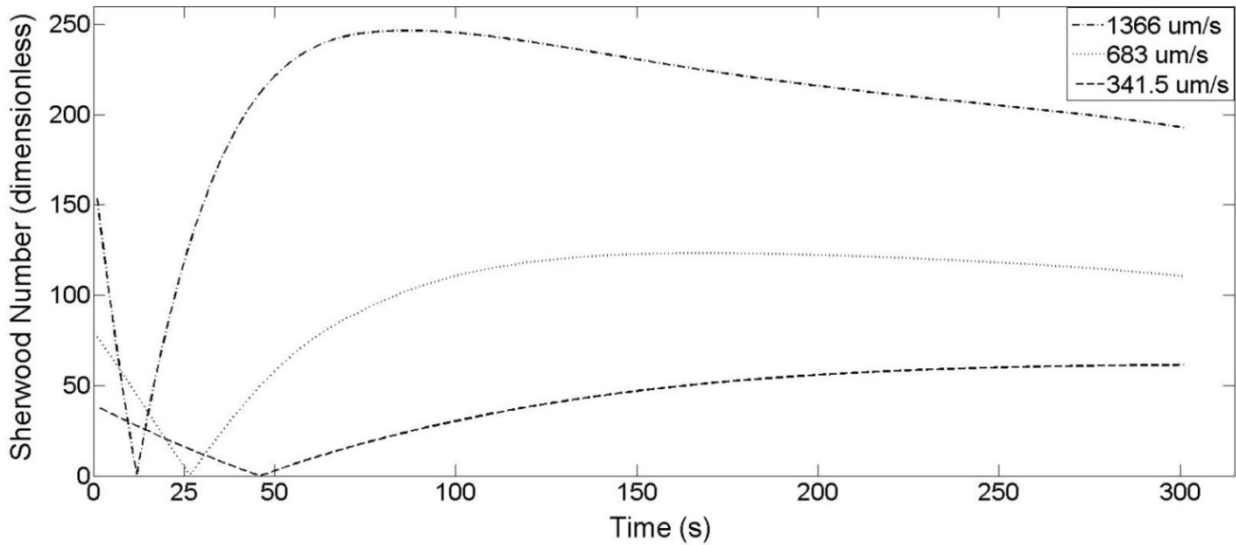
Figure-4.13. Sherwood Number for comparison of convective and diffusive flux at various flow rates.

4.4 Optimization of the Results

Values of droplet radius between R=42.5µm and R=20µm found as optimum rate interval. In this interval, the rate of transfer of water into the organic phase is at maximum. If pre-concentration process is operated with 85 micron droplets, a faster increase in the CPA concentration can be achieved. Also Rcritical region will be avoided (see **figure-4.14**).
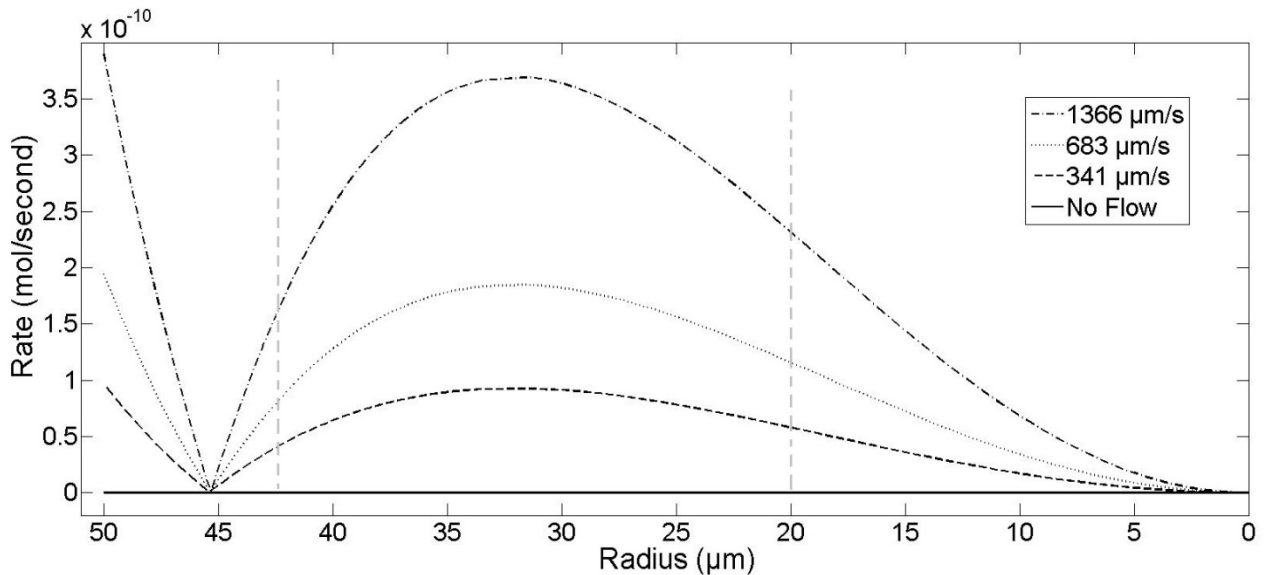
Figure-4.14. The rate of water transfer to organic phase with respect to droplet radius. Dashed light gray lines represent optimum intervals.

It is shown on **Figure-4.4** that it only takes 140 seconds to reduce droplet radius from 42.5µm to 20 µm at 1366µm/s flow rate. That is enough reduction to achieve 9.5 times the initial CPA concentration. If 683µm/s flow rate is applied, it would take 240 seconds to achieve the same pre-concentration rate. **Figure-4.15** summarizes the time needed to achieve certain CPA concentration if starting droplet radius is chosen as 42.5µ.
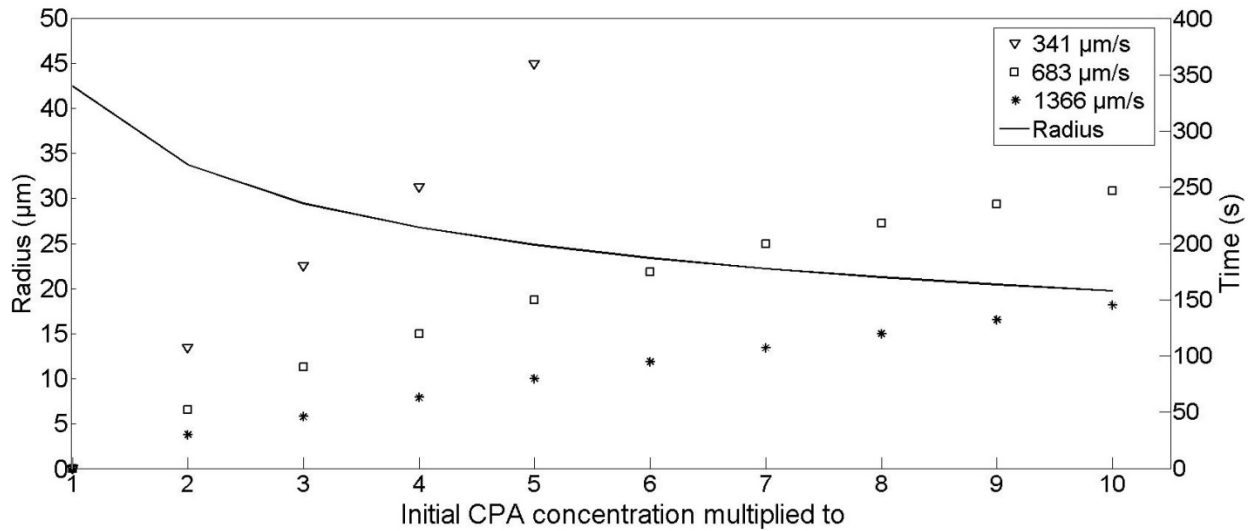
Figure-4.15. Time required to reach multiplies of initial CPA concentration for 85 micron initial droplet size (R=42.5 µm).

According to the results, theoretically, at 683 µm/s and 1366 µm/s flow rates, it is possible to pre-concentrate cells with CPA in less than 300 seconds (see **figure-4.15**). If possible, the flow rate can be increased as needed to achieve faster pre-concentration. Higher flow rate of organic phase is always yielding higher CPA concentrations within droplets while decreasing process time. If working with highly sensitive cells is needed, lower initial concentration of CPA can be chose to prevent CPA toxicity on the cell while increasing the flow rate as much as possible. Nevertheless, membrane permeability (Ps) stands as a limiting value for mass transfer into the cell, if the CPA concentration is increased in 1:10 ratio under 300 seconds, there may be an accumulation of CPA molecules over the cell membrane surface causing osmotic injury to the cell.

5. CONCLUSIONS

- Increasing the average organic phase flow rate enhances the mass transfer rate from droplet to organic phase.

- Theoretically, it is possible to achieve 10 times the initial concentration by reducing droplet size in a microchannel in less than 150 seconds. However, membrane permeability (Ps) stands as a limiting value for mass transfer into the cell. If the CPA concentration is increased in such rate, there may be an accumulation of CPA molecules over the cell membrane surface. Special care might be needed especially for membranes with low Ps value. Concentration should always be increased in a matched rate of diffusion through cell membrane, a rate that would not cause the cells to give responses as they would to high concentration differences around the cell. Effectiveness of the method can be lost due to response of the cell to high CPA concentration difference in and out of the cell. If accumulation is at stake, mild temperature increase rate can be preferred over sudden temperature increase on microfluidic system for controlling the mass transfer rate.

- Apart from the discussions on the vagueness of the reflection coefficient, there is a certain need for a model, which fully describes the biological responses of the cells. There is not any adequate model, independent of the experimental data, describing cell response (shrinking or swelling of cells) to concentration changes. Without using any experimental data, currently available models are only good for approximate predictions using the 'constant cell volume' assumption or 'the intracellular CPA concentration independent of cell volume' assumption for cells. By doing the mentioned assumptions, we calculated the cell response to our CPA concentration values and we found mild cell responses as cell shrink to %85 its volume in 240 seconds, if $Ps=8x10^{-7}$ and cell shrink to 98% its volume in 240 seconds, if $Ps=8x10^{-6}$.

- In order to achieve maximized pre-concentration with droplets, Critical Radius value should be avoided by choosing appropriate channel width. Ideally, for a channel with 150x200μm cross section, droplets smaller than 90 micron should be generated.

- Soybean oil is a non-toxic and low cost organic phase, but water solubility of soybean oil is very limited. Fatty alcohols having 8 carbons to 12 carbons in their chains are capable of

solving water up to 5% w/w. Those substances should be examined for use in pre-concentration of cells via aqueous droplets.

- Flow characteristics, the dragging of the droplets, and thus the droplet position can be examined more precisely by accounting for drag force acting on the droplets.

- In our research we created an insight to understand the flow dynamics and mass transfer in microfluidic devices better for droplets generated in micro-channels. There are many applications available with multiple phase flows, electromagnetically driven flows and concentration control with optical vertex (Squires and Bazant 2004, Jeffries, Kuo et al. 2007). We highly encourage any reader to search for MEMS and BioMEMS through literature to understand the possible uses and impacts of these devices in the future.

6. REFERENCES

Acker, J. P. (2007). "Biopreservation of Cells and Engineered Tissues." **103**: 157-187.

Bajpayee, A., et al. (2010). "Concentration of glycerol in aqueous microdroplets by selective removal of water." <u>Anal Chem</u> **82**(4): 1288-1291.

Beebe, D. J., et al. (2002). "Physics and applications of microfluidics in biology." <u>Annu Rev Biomed Eng</u> **4**: 261-286.

Bruce Alberts, A. J. (2008). <u>Molecular Biology of the Cell</u>, Garland Science.

Chiu, D. T. (2007). Aqueous Droplets as Single-Molecule Reaction Containers. <u>The 14th International Conference on Solid-State Sensors, Actuators and Microsystems</u>. Lyon, France, Transducers & Eurosensors.

Chiu, D. T. and R. M. Lorenz (2009). "Chemistry and biology in femtoliter and picoliter volume droplets." <u>Acc Chem Res</u> **42**(5): 649-658.

Chiu, D. T., et al. (2009). "Droplets for ultrasmall-volume analysis." <u>Anal Chem</u> **81**(13): 5111-5118.

Crowe, J. H. and L. M. Crowe (2000). "Preservation of mammalian cells-learning nature's tricks." <u>Nat Biotechnol</u> **18**(2): 145-146.

Cui, Z. F., et al. (2002). "Modeling of cryopreservation of engineered tissues with one-dimensional geometry." <u>Biotechnol Prog</u> **18**(2): 354-361.

Czaplewski, D. A., et al. (2003). "Nanofluidic channels with elliptical cross sections formed using a nonlithographic process." <u>Applied Physics Letters</u> **83**(23): 4836.

Dittrich, P. S. and A. Manz (2006). "Lab-on-a-chip: microfluidics in drug discovery." <u>Nat Rev Drug Discov</u> **5**(3): 210-218.

Elmoazzen, H. Y., et al. (2009). "Osmotic transport across cell membranes in nondilute solutions: a new nondilute solute transport equation." <u>Biophys J</u> **96**(7): 2559-2571.

Elvira, K. S., et al. (2013). "The past, present and potential for microfluidic reactor technology in chemical synthesis." <u>Nat Chem</u> **5**(11): 905-915.

Eroglu, A., et al. (2000). "Intracellular trehalose improves the survival of cryopreserved mammalian cells." Nat Biotechnol **18**(2): 163-167.

Geankoplis, C. J. (2003). Transport Processes and Separation Process Principles (Includes Unit Operations), Prentice Hall Professional Technical Reference.

Hammerstedt, R. H., et al. (1990). "Cryopreservation of Mammalian Sperm - What We Ask Them to Survive." Journal of Andrology **11**(1): 73-88.

He, M., et al. (2005). "Selective encapsulation of single cells and subcellular organelles into picoliter- and femtoliter-volume droplets." Anal Chem **77**(6): 1539-1544.

He, M., et al. (2004). "Concentrating solutes and nanoparticles within individual aqueous microdroplets." Anal Chem **76**(5): 1222-1227.

Heo, Y. S., et al. (2011). "Controlled loading of cryoprotectants (CPAs) to oocyte with linear and complex CPA profiles on a microfluidic platform." Lab Chip **11**(20): 3530-3537.

Ho, C.-T., et al. (2006). "Rapid heterogeneous liver-cell on-chip patterning via the enhanced field-induced dielectrophoresis trap." Lab Chip **6**(6): 724-734.

Hou, T. and Y. Efendiev (2009). Multiscale Finite Element Methods. Theory and Applications, New York, NY : Springer New York, 2009.

Illmer P, E. C., Schinner F. (1999). "A practicable and accurate method to differentiate between intra- and extracellular water of microbial cells." FEMS Microbiol Lett.

Jacobs M. H., D. R. S. (1932). "A Simple Method for the Quantitative Measurement of Cell Permeability." Journal of Cell. Comp. Physiol.: 71-82.

Jacobs, M. H. (1933). "The Simultaneous Measurement of Cell Permeability to Water and to Dissolved Substances." Journal of Cell. Comp. Physiol **2**: 427-444.

Janasek, D., et al. (2006). "Scaling and the design of miniaturized chemical-analysis systems." Nature **442**(7101): 374-380.

Jeffries, G. D., et al. (2007). "Controlled shrinkage and re-expansion of a single aqueous droplet inside an optical vortex trap." J Phys Chem B **111**(11): 2806-2812.

Jeffries, G. D., et al. (2007). "Dynamic modulation of chemical concentration in an aqueous droplet." Angew Chem Int Ed Engl **46**(8): 1326-1328.

Jerry W. King, G. R. (1996). "Supercritical fluid technology in oil and lipid chemistry." American Oil Chemists' Society: 303.

Jessamine M. K. Ng, I. G., Abraham D. Stroock, George M. Whitesides (2002). "Components for integrated poly(dimethylsiloxane) microfluidic systems." Electrophoresis **23**: 3461–3473.

Kedem, O. (1961). "A Physical Interpretation of the Phenomenological Coefficients of Membrane Permeability." The Journal of General Physiology **45**(1): 143-179.

Kedem, O. and A. Katchalsky (1958). "Thermodynamic analysis of the permeability of biological membranes to non-electrolytes." Biochim Biophys Acta **27**(2): 229-246.

Kenis, P. J. (1999). "Microfabrication Inside Capillaries Using Multiphase Laminar Flow Patterning." Science **285**(5424): 83-85.

Kleinhans, F. W. (1998). "Membrane permeability modeling: Kedem-Katchalsky vs a two-parameter formalism." Cryobiology **37**(4): 271-289.

Kuo, J. S. and D. T. Chiu (2011). "Controlling mass transport in microfluidic devices." Annu Rev Anal Chem (Palo Alto Calif) **4**: 275-296.

Lagus, T. P. and J. F. Edd (2013). "A review of the theory, methods and recent applications of high-throughput single-cell droplet microfluidics." Journal of Physics D: Applied Physics **46**(11): 114005.

Li, L.-y. (2006). "Numerical simulation of mass transfer during the osmotic dehydration of biological tissues." Computational Materials Science **35**(2): 75-83.

M. Toner, A. A. (2005). Roles of Thermodynamic State and Molecular Mobility in Biopreservation. Tissue Engineering and Artificial Organs, CRC Press**:** 1-20.

Maczynski, A., et al. (2007). "IUPAC-NIST Solubility Data Series. 82. Alcohols with Water–Revised and Updated: Part 5. C[sub 8]–C[sub 17] Alcohols with Water." Journal of Physical and Chemical Reference Data **36**(3): 685.

Meryman, H. T. (1971). "Cryoprotective agents." Cryobiology **8**(2): 173-183.

Michael J. Taylor, Y. C. S., Kelvin G.M. Brockbank (2004). "Vitrification in Tissue Preservation: New Developments." 603-641.

Mijatovic, D., et al. (2005). "Technologies for nanofluidic systems: top-down vs. bottom-up--a review." Lab Chip **5**(5): 492-500.

Palasz, A. T. and R. J. Mapletoft (1996). "Cryopreservation of mammalian embryos and oocytes: recent advances." Biotechnol Adv **14**(2): 127-149.

Prot, J.-M., et al. (2012). "Predictive toxicology using systemic biology and liver microfluidic "on chip" approaches: Application to acetaminophen injury." Toxicology and Applied Pharmacology **259**(3): 270-280.

Pryor, R. W. (2011). Multiphysics Modeling Using COMSOL® v.4, Jones and Bartlett Publishers.

Purcell, E. M. (January 1977). "Life at low Reynolds number." American Journal of Physics **45**(1).

R. Byron Bird, W. E. S., Edwin N. Lightfoot (2006). Transport Phenomena, Wiley.

Rubinsky, B. (2003). "Principles of low temperature cell preservation." Heart Fail Rev **8**(3): 277-284.

S. Matsuo, T. M. (1989). "Viscosities of Six 1-Alkanols at Temperatures in the Range 298-348 K and Pressures up to 200 MPa." International Journal of Thermophysics **10**(4).

Santiago, J. G. (2001). "Electroosmotic Flows in Microchannels with Finite Inertial and Pressure Forces." Anal. Chem. **73**: 2353-2365.

Sgro, A. E. and D. T. Chiu (2010). "Droplet freezing, docking, and the exchange of immiscible phase and surfactant around frozen droplets." Lab Chip **10**(14): 1873-1877.

Sjostrom, S. L., et al. (2014). "High-throughput screening for industrial enzyme production hosts by droplet microfluidics." Lab Chip **14**(4): 806-813.

Song, Y. S., et al. (2009). "Microfluidics for cryopreservation." Lab Chip **9**(13): 1874-1881.

Squires, T. M. and M. Z. Bazant (2004). "Induced-charge electro-osmosis." Journal of Fluid Mechanics **509**: 217-252.

Squires, T. M. and S. R. Quake (2005). "Microfluidics: Fluid physics at the nanoliter scale." <u>Reviews of Modern Physics</u> **77**(3): 977-1026.

Staverman, A. J. (1952). "Non-equilibrium thermodynamics of membrane processes." <u>Transactions of the Faraday Society</u> **48**: 176.

Stone, H. A. and S. Kim (2001). "Microfluidics: Basic issues, applications, and challenges." <u>AIChE Journal</u> **47**(6): 1250-1254.

Stroock, A. D., et al. (2002). "Chaotic mixer for microchannels." <u>Science</u> **295**(5555): 647-651.

Swain, J. E., et al. (2013). "Thinking big by thinking small: application of microfluidic technology to improve ART." <u>Lab Chip</u> **13**(7): 1213-1224.

Teh, S.-Y., et al. (2008). "Droplet microfluidics." <u>Lab on a Chip</u> **8**(2): 198.

Ternström, G., et al. (1996). "Mutual Diffusion Coefficients of Water + Ethylene Glycol and Water + Glycerol Mixtures." <u>Journal of Chemical & Engineering Data</u> **41**(4): 876-879.

Toner, M., et al. (1990). "Thermodynamics and Kinetics of Intracellular Ice Formation during Freezing of Biological Cells." <u>Journal of Applied Physics</u> **67**(3): 1582-1593.

Tong Wang, P. J. W. (2005). Soybean Oil. <u>Bailey's Industrial Oil and Fat Products</u>. F. Shahidi., John Wiley & Sons, Inc.**:** 577-653.

Vian, A. M. and A. Z. Higgins (2014). "Membrane permeability of the human granulocyte to water, dimethyl sulfoxide, glycerol, propylene glycol and ethylene glycol." <u>Cryobiology</u> **68**(1): 35-42.

Weibel, D. B. and G. M. Whitesides (2006). "Applications of microfluidics in chemical biology." <u>Curr Opin Chem Biol</u> **10**(6): 584-591.

Whitesides, G. M. (2006). "The origins and the future of microfluidics." <u>Nature</u> **442**(7101): 368-373.

Xia, Y. and G. M. Whitesides (1998). "Soft Lithography." <u>Annual Review of Materials Science</u> **28**(1): 153-184.

Yamaji, Y., et al. (2006). "Cryoprotectant permeability of aquaporin-3 expressed in Xenopus oocytes." <u>Cryobiology</u> **53**(2): 258-267.

Youm, H. W., et al. (2014). "Optimal vitrification protocol for mouse ovarian tissue cryopreservation: effect of cryoprotective agents and in vitro culture on vitrified-warmed ovarian tissue survival." <u>Hum Reprod</u> **29**(4): 720-730.

7. APPENDIX

7.1 Possible Organic Phase Substances

	Dodecanol		Undecanol		Decanol			Nonanol			2-Ethyl Hexanol		Ocatanol			Cyclooctanol		Soybean Oil
Temperature (°C)	30	40	20	40	20	30	40	20	30	40	20	40	20	30	40	30	40	25
Water Solubility w%	2.87	2.85	3.21	3.09	3.68	3.35	3.48	3.68	3.92	3.94	2.4	2.72	4.35	4.48	4.81	5.18	5.49	0.4
Solubility in Water w%	0.04	0.05	0.03	0.09	0.021		0.026		0.031	0.034	0.125	0.11	0.049		0.065	0.61	0.6	-
Viscosity (mPa.s)	15.91		17.2		11.05			11.7			9.8		10.6			136		58 - 62
Density (g/cm3)	0.8309		0.8298		0.8297			0.8279			0.8344		0.827			0.97		0.917
Melting p. Boiling p. (°C)	24 259		19 243		6.4 232			- 5 213			-76 184		- 16 196			15 105		0.6 >260
Toxicity	Non - Hazardous Toxic to aquatic life		Non - Hazardous Toxic to aquatic life		Non - Hazardous			Toxic by Inhalation Toxic to aquatic life			Target Organ Effects		Non - Hazardous Toxic to aquatic life			Non - Hazardous or Not investigated		Non-Hazardous
Ref.	**Solubility**: (Maczynski, Shaw et al. 2007) **Viscosity:** (S. Matsuo 1989), (Tong Wang 2005) **Other references from** (data vary depending on the purity and the manufacturer) 1-United States Library of Medicine – Toxicology Data Network. 2- Sigma Aldrich MSDS forms.																	

7.2　Parameters and Variables Used in the Comsol Model

7.2.1　An Apparence of the Comsol Model Building Panel

7.2.2 Comsol Parameters and Variables for No Flow condition

▼ Parameters

Name	Expression	Value
R0	0.000050	5.00000000000000E-5
V0	(4/3)*pi*R0^3[m^3]	5.23598775598299E-13 m³
A0	4*pi*R0^2[m^2]	3.14159265358979E-8 m²
W	0.000150[m]	1.50000000000000E-4 m
Mu_oil	0.05[kg/(m*s)]	0.0500000000000000 kg/(m·s)
L	0.35[m]	0.350000000000000 m
Lin_U	0.000683[m/s]	6.83000000000000E-4 m/s
Avg_U_over_DeltaP	0.00000011338095238[m^2*s/(kg)]	1.13380952380000E-7 m²·s/kg
mol_CPA	0.5[mol/liter]	500.000000000000 mol/m³
Slip_velocity	Lin_U*0.1	6.83000000000000E-5 m/s
C_initial_wtr_in_oil	45.75[mol/m^3]	45.7500000000000 mol/m³
C_final_wtr_in_oil	73.15[mol/m^3]	73.1500000000000 mol/m³

▼ Variables

Name	Expression	Unit
Ri	((0.00000006*t^3[1/s^3] - 0.00008*t^2[1/s^2] + 0.0006*t[1/s]+50)*1e-6)[m]	m
Vi	(4/3)*pi*Ri^3	m³
Ai	4*pi*Ri^2	m²
DeltaP	Lin_U/Avg_U_over_DeltaP	Pa
U_over_DeltaP	-((Ri^2-(W^2)/4)/(L*Mu_oil*2))	m²·s/kg
Ui	DeltaP*U_over_DeltaP	m/s
Ui_with_slip	Ui+Slip_velocity	m/s
DeltaU	Ui_with_slip-Lin_U	m/s
percnt_change_V	Vi/V0	
c_CPA	mol_CPA/percnt_change_V	mol/m³
MeshVelocity	((0.00000018*t^2[1/s^2]-0.00016*t[1/s] + 0.0006)*1e-6)[m/s]	m/s

7.2.3 Comsol Parameters and Variables for 341,5 µm/s average flow velocity

Parameters

Name	Expression	Value
R0	0.000050	5.00000000000000E-5
V0	(4/3)*pi*R0^3[m^3]	5.23598775598299E-13 m³
A0	4*pi*R0^2[m^2]	3.14159265358979E-8 m²
W	0.000150[m]	1.50000000000000E-4 m
Mu_oil	0.05[kg/(m*s)]	0.0500000000000000 kg/(m·s)
L	0.35[m]	0.350000000000000 m
Lin_U	0.0003415[m/s]	3.41500000000000E-4 m/s
Avg_U_over_DeltaP	0.00000011338095238[m^2*s/(kg)]	1.13380952380000E-7 m²·s/kg
mol_CPA	0.5[mol/liter]	500.000000000000 mol/m³
Slip_velocity	Lin_U*0.1	3.41500000000000E-5 m/s
C_initial_wtr_in_oil	45.75[mol/m^3]	45.7500000000000 mol/m³
C_final_wtr_in_oil	73.15[mol/m^3]	73.1500000000000 mol/m³

Variables

Name	Expression	Unit
Ri	Ri1	m
Ri1	((0.0000001*t^3[1/s^3] + 0.00008*t^2[1/s^2] - 0.1081*t[1/s]+50)*1e-6)[m]	m
Ri2	((-0.00000123*t^3[1/s^3]+0.0009*t^2[1/s^2]-0.2685*t[1/s]+101.662)*0.5e-6)[m]	m
Vi	(4/3)*pi*Ri^3	m³
Ai	4*pi*Ri^2	m²
DeltaP	Lin_U/Avg_U_over_DeltaP	Pa
U_over_DeltaP	-((Ri^2-(W^2)/4)/(L*Mu_oil*2))	m²·s/kg
Ui	DeltaP*U_over_DeltaP	m/s
Ui_with_slip	Ui+Slip_velocity	m/s
DeltaU	Ui_with_slip-Lin_U	m/s
percnt_change_V	Vi/V0	
c_CPA	mol_CPA/percnt_change_V	mol/m³
MeshVelocity	MeshVelocity1	m/s
MeshVelocity1	(0.0000003*t^2[1/s^2] + 0.00016*t[1/s] - 0.1081)*1e-6[m/s]	m/s
MeshVelocity2	(-0.00000369*t^2[1/s^2]+0.0018*t[1/s]-0.2685)*0.5e-6[m/s]	m/s

7.2.4 Comsol Parameters and Variables for 683 μm/s average flow velocity

Parameters

Name	Expression	Value
R0	0.000050	5.00000000000000E-5
V0	(4/3)*pi*R0^3[m^3]	5.23598775598299E-13 m³
A0	4*pi*R0^2[m^2]	3.14159265358979E-8 m²
W	0.000150[m]	1.50000000000000E-4 m
Mu_oil	0.05[kg/(m*s)]	0.0500000000000000 kg/(m·s)
L	0.35[m]	0.350000000000000 m
Lin_U	0.000683[m/s]	6.83000000000000E-4 m/s
Avg_U_over_DeltaP	0.00000011338095238[m^2*s/(kg)]	1.13380952380000E-7 m²·s/kg
mol_CPA	0.5[mol/liter]	500.000000000000 mol/m³
Slip_velocity	Lin_U*0.1	6.83000000000000E-5 m/s
C_initial_wtr_in_oil	45.75[mol/m^3]	45.7500000000000 mol/m³
C_final_wtr_in_oil	73.15[mol/m^3]	73.1500000000000 mol/m³

Variables

Name	Expression	Unit
Ri	Ri1*(t<71.306)+Ri2*(t>=71.306)	m
Ri1	((0.0000175*t^3[1/s^3] - 0.0018*t^2[1/s^2]- 0.1479*t[1/s]+50)*1e-6)[m]	m
Ri2	((-0.00000123*t^3[1/s^3]+0.0009*t^2[1/s^2] - 0.2685*t[1/s]+51.692)*1e-6)[m]	m
Vi	(4/3)*pi*Ri^3	m³
Ai	4*pi*Ri^2	m²
DeltaP	Lin_U/Avg_U_over_DeltaP	Pa
U_over_DeltaP	-((Ri^2-(W^2)/4)/(L*Mu_oil*2))	m²·s/kg
Ui	DeltaP*U_over_DeltaP	m/s
Ui_with_slip	Ui+Slip_velocity	m/s
DeltaU	Ui_with_slip-Lin_U	m/s
percnt_change_V	Vi/V0	
c_CPA	mol_CPA/percnt_change_V	mol/m³
MeshVelocity	MeshVelocity1*(t<71.306)+MeshVelocity2*(t>=71.306)	m/s
MeshVelocity1	(0.000054*t^2[1/s^2]- 0.0036*t[1/s]- 0.1479)*1e-6[m/s]	m/s
MeshVelocity2	(-0.00000369*t^2[1/s^2]+0.0018*t[1/s] - 0.2685)*1e-6[m/s]	m/s

7.2.5 Comsol Parameters and Variables for 1366 μm/s average flow velocity

Parameters

Name	Expression	Value
R0	0.000050	5.00000000000000E-5
V0	(4/3)*pi*R0^3[m^3]	5.23598775598299E-13 m³
A0	4*pi*R0^2[m^2]	3.14159265358979E-8 m²
W	0.000150[m]	1.50000000000000E-4 m
Mu_oil	0.05[kg/(m*s)]	0.0500000000000000 kg/(m·s)
L	0.35[m]	0.350000000000000 m
Lin_U	0.001366[m/s]	0.00136600000000000 m/s
Avg_U_over_DeltaP	0.00000011338095238[m^2*s/(kg)]	1.13380952380000E-7 m²·s/kg
mol_CPA	0.5[mol/liter]	500.000000000000 mol/m³
Slip_velocity	Lin_U*0.1	1.36600000000000E-4 m/s
C_initial_wtr_in_oil	45.75[mol/m^3]	45.7500000000000 mol/m³
C_final_wtr_in_oil	73.15[mol/m^3]	73.1500000000000 mol/m³

Variables

Name	Expression	Unit
Ri	Ri1*(t<73.48)+Ri2*(t>=73.48)	m
Ri1	((0.002*t^2[1/s^2]-0.4498*t[1/s]+50)*1e-6)[m]	m
Ri2	((-0.0000012*t^3[1/s^3]+0.0009*t^2[1/s^2]-0.2496*t[1/s]+41.704)*1e-6)[m]	m
Vi	(4/3)*pi*Ri^3	m³
Ai	4*pi*Ri^2	m²
DeltaP	Lin_U/Avg_U_over_DeltaP	Pa
U_over_DeltaP	-((Ri^2-(W^2)/4)/(L*Mu_oil*2))	m²·s/kg
Ui	DeltaP*U_over_DeltaP	m/s
Ui_with_slip	Ui+Slip_velocity	m/s
DeltaU	Ui_with_slip-Lin_U	m/s
percnt_change_V	Vi/V0	
c_CPA	mol_CPA/percnt_change_V	mol/m³
MeshVelocity	MeshVelocity1*(t<73.48)+MeshVelocity2*(t>=73.48)	m/s
MeshVelocity1	(0.004*t[1/s]-0.4498)*1e-6[m/s]	m/s
MeshVelocity2	(-0.0000036*t^2[1/s^2]+ 0.0018*t[1/s]-0.2496)*1e-6[m/s]	m/s

7.3 Apparences of Some Excel Sheets

Excel spreadsheet — Home ribbon

Cell reference: V44 | Formula bar: `= =0,000035*P44^2 - 0,0036*P44 - 0,1479`

Column headers:

B — Ri in micrometers	D — R0	E — Flux (mol/m2,s)	F — R critical (m)	H — Flux (fitted values)	I — Flux (fitted)	K — Flux (fitted values) microns	L — Flux (fitted values) microns	N — Ri larger than 45,33	O — Ri smaller than 45,33	P — Time in one column (sec)	Q — Area (m^2)	R — Rate (mol/s)	S — Ri fitted eq	T — Ri fitted eq. in micrometers

Selected readable values:

Column B (Ri in micrometers):
50,000000; 49,879764; 49,536463; 49,015307; 48,373488; 47,665424; 46,934625; 46,211832; 45,516646; 45,330000; 44,860266; 44,248088; 43,681741; 43,160541; 43,100000; 43,045679; 42,889088; 42,647315; 42,343309; 42,000679; 41,640500; 41,277440; 40,924147; 40,587433; 40,271454; 39,978146; 39,900000; 38,873025; 39,794896; 39,673249; 39,518665; 39,342498; 39,155151; 38,965117; 38,600175; 38,432149; 38,275972; 38,200000; 38,186716; 38,148141; 38,087798; 38,010660; 37,922195; 37,827555

Column T (Ri fitted eq. in micrometers):
50; 49,8864352; 49,5593668; 49,0973934; 48,3878117; 47,65670863; 46,9603646; 46,17066469; 45,4787588; 45,29637657; 44,83916876; 44,2445794; 43,6945253; 43,18737016; 43,1288666; 43,0754871; 42,92275129; 42,68670824; 42,38933045; 42,05338532; 41,69884611; 41,34186832; 40,99220936; 40,65575588; 40,34359966; 40,05423583; 39,97665114; 39,94985999; 39,87230144; 39,75156833; 39,59819694; 39,42354289; 39,23801169; 39,05017169; 38,86630176; 38,69072042; 38,5258724; 38,37340826; 38,29441232; 38,2849866; 38,24899069; 38,19042029; 38,11569003; 38,03022556; 37,93908894

Column P (Time in one column (sec)):
0,0000; 0,7608; 2,9028; 6,0706; 9,8354; 13,8185; 17,7474; 21,4570; 24,8643; 25,7330; 27,9643; 30,8186; 33,3464; 35,8659; 36,1475; 36,4003; 37,1299; 38,2593; 39,6859; 41,3043; 43,0225; 44,7684; 46,4897; 48,1513; 49,7315; 51,2180; 51,6175; 51,7558; 52,1572; 52,7852; 53,5888; 54,5124; 55,5042; 56,5205; 57,5282; 58,5034; 59,4308; 60,3014; 60,7279; 60,8027; 61,0202; 61,3615; 61,7998; 62,3051; 62,8489

Note: This page is a dense numerical spreadsheet. Additional columns (D, E, F, H, I, K, L, N, O, Q, R, S) contain long-precision numeric data not fully transcribed.

7.4 A Matlab Function written to be called by Comsol

```matlab
function vrble_iteration = A(R0,t,Total_flux)
R0=0.00005;
t=0;
Total_flux=0.005;
Ri = (1./3).*(((((3^(4./3)).*(27.*(R0^6)-4.*R0^3.*((Total_flux.*27.*1e-
6)^3).*t^6)^(0.5)+27.*R0^3-2.*((Total_flux.*27.*1e-
6)^3).*t^6)./2)^(1./3)+(((2^(1./3))*((Total_flux.*27.*1e-
6)^(2)).*t^4)./((3^(4./3)).*(27.*(R0^6)-4.*(R0^3)*((Total_flux.*27.*1e-
6)^3).*t^6)^(0.5)+27.*(R0^3)-2.*((Total_flux.*27.*1e-6)^3).*t^6)^(1./3))-
Total_flux.*27.*1e-6.*t^2)
end
```

where, 'Ri' is the variable to be read by Comsol.

CURRICULUM VITAE

Credentials

Name, Surname: Ufuk Okumuş

Place of Birth: Ankara

Marital Status: Single

E-mail: ufukokumus@gmail.com

Address**:** Yeşilada sitesi 8. Cad. 2651. Sok. 5/4, Çayyolu / ANKARA

Education

High School: Gölbaşı Anadolu Lisesi

BSc. : Hacettepe University, Chemical Engineering

MSc. : Hacettepe University, Chemical Engineering

Foreign Languages

English

Work Experience

Imtek Cryogenics, Thermodynamic Modeling of Cryocoolers.

Areas of Experiences

Chemical Engineering, Research & Development, Finite Element Analysis, Microfluidics, Cryopreservation, Transport Phenomena

Projects and Budgets

Finite Element Analysis Modeling, Scientific Research Projects Coordination Unit of Hacettepe University, 12600 TL

Publications

-

Oral and Poster Presentations

Ufuk Okumus (presenter), Selis Onel, "Uniform Aqueous Droplets in a Thermal Micro-Fluidic System Designed for Biopreservation", Poster presentation, 06.2013 TERMIS-EU international conference, Harbiye Convention Center, Istanbul